CENTRO DE INVESTIGACIONES
EN OPTICA, A.C.

“VECTOR VORTEX HOLOGRAPHIC GRATINGS INSCRIBED IN AZOBENZENE-CONTAINING POLYMER FILMS AND ITS DIFFRACTION FEATURES”

Thesis to obtain the degree of Master of Science (Optics)

Presents: Dixie Leilany Medina Espíritu, B. Eng

Thesis director: Geminiano Donaciano Martínez-Ponce, Ph. D.

Co-advisor: Rosa Julia Rodríguez González, M.Sc.

León · Guanajuato · México
December 2024

Dedicated to

God

my mother,
Leticia Espíritu

my father,
Francisco Medina

and
my sister
Halia Medina

ACKNOWLEDGEMENTS

First and foremost, I would like to express my deepest gratitude to my supervisor, Geminiano Donaciano Martínez Ponce, Ph. D., and my co-advisor, Rosa Julia Rodríguez González, M. Sc. for the continuous support of my study and research, for their patience, motivation, enthusiasm, and immense knowledge. Their guidance helped me in all the time of research and writing of this thesis. I could not have imagined having better advisors and mentors for my formation.

Likewise I thank Leticia Larios López Ph. D. and Isaura Félix, Ph. D. for receiving me in their laboratory and showing me different ways of working, and for making me feel at home being in a faraway place.

I thank my investigation group: Oscar, Enrique, Danay, Yanier, Jaiver, Ana and Miguel Ángel for the stimulating discussions, for sharing ideas and knowledge, for all the fun we have had in the last 2 years and the most important, for the feedback during our presentations.

Also, I thank my friends Ingrid and Oscar for their support and encouragement, and for those trips and memories we share.

I am also grateful to Centro de Investigaciones en Óptica (CIO) for providing the necessary facilities and funding that enabled me to complete this research. To Centro de Investigación en Química Aplicada (CIQA) for allowing me to do my research stay and continue my project.

I would like to thank my thesis committee: Geminiano Martínez, Ph. D., Leticia Larios López, Ph. D., and Alma Adriana Camacho Pérez, Ph. D., for their insightful comments and encouragement, but also for the hard questions which encourage me to widen my research from various perspectives. And, finally, I thank CONAHCyT for the scholarship granted over these two years, and also for the financial support on the project CF-2023-I-2503.

I must express my very profound gratitude to my parents and my family for providing me with unfailing support and continuous encouragement throughout my years of study and through the process of researching and writing this thesis. This accomplishment would not have been possible without them. Thank you.

Dixie Leilany Medina Espíritu
Date: 11/2024

ABSTRACT

Anisotropic optical response of azobenzene-containing polymer thin films when exposed to spatially modulated polarization fields has been investigated for a long time. Besides a locally photo-induced birefringence and diattenuation due to molecular reorientation, the photo-responsive film also experiences an electric field gradient force that shapes the surface. These unique features allow the simultaneous recording of polarization and surface-relief gratings, as well as the development of polarization-sensitive diffractive elements. In the first stage of this thesis project, photo-reactive films made with a new azopolymer series is characterized by Stokes polarimetry with the aim of analyzing the photo-induced orientation dynamics. Then, polarization (vector) holographic gratings resulting from superposition of radial and azimuthal linearly polarized fields are recorded in the azopolymer films and studied by Mueller imaging polarimetry. Finally, diffracted vector fields in hologram reconstruction stage are analyzed using Stokes imaging polarimetry. The multiplexing capacity of the holographic recording medium open the way to develop hereafter an analyzer device of optical vector beams.

Keywords: Vector holography, photo-induced birefringence, Stokes polarimetry, azobenzene-containing polymer

Contents

List of Figures

List of Tables

Chapter 1

Introduction

1.1 Background

Photoinduced anisotropy using polarized light in thin photosensitive films was first reported by Fritz Weigert in silver-halide films in 1919 and, since then, it is also known as Weigert effect.[1] Later, T. Kondo observed this interesting outcome when gelatin films sensitized with an azobenzene dye were illuminated with ultraviolet linearly polarized light.[2] However, while the physical mechanism involved in the former is mainly an anisotropic absorption (dichroism or diattenuation), in the latter it is a molecular photoinduced alignment that is predominantly observed as birefringence. The first report on the possibility of vector wavefront recording and reconstruction is due to Adolf W. Lohman.[3] This was accomplished for the first time in 1972, when Shermazan D. Kakichashvili implemented the particular processes of polarization holographic gratings obtained by superposition of reference and object waves with orthogonal states of polarization, specifically the cases of linearly and circularly polarized beams.[4]

Potential applications of Weigert effect in vector diffractive holographic elements have stimulated the design and synthesis of new smart light-responsive materials with the aim of optimizing the hologram diffraction efficiency, namely, the birefringence modulation depth.[5] Photoinduced molecular orientation in azobenzene containing polymer films is an interesting research frontier fostered by unique physical and chemical mechanisms, which triggers the recording, detecting, manipulating, and reconstructing of polarized fields based on polarization holograms. [6, 7] The most basic holographic storage media consists in azobenzene units dispersed into a polymer host, such as polyethylene glycol (PEG); however, that systems have shown poor diffraction efficiency. [8, 9]

On the other hand, through out polymer synthesis engineering, it is possible the

insertion of azobenzene units into the polymer-matrix main chain or to attach them sideways.[10] Nonetheless, because the required molecular mobility to obtain optical anisotropy and solubility facts, the latter structure is often found in applications. The polymer phase, amorphous or liquid-crystalline, depends significantly on the spacer length between the main chain and the azobenzene mesogen.[11] On the other hand, absorbance peaks are defined by the molecular conjugation that depends on the push-pull donor and acceptor groups on the opposite sides of the benzene rings.[12]

In the research group on Polarized Light and Photoacoustics in Centro de Investigaciones en Óptica (CIO), in collaboration with researchers of the Advanced Materials Department in Centro de Investigación en Química Aplicada (CIQA), a number of side-chain azobenzene-containing polymers has been synthesized and characterized.[13, 14, 15, 16] Also, optical devices have been proposed exploiting their polarization attributes.[17, 18, 19] Polarimetric devices developed in our group, such as a Mueller and Stokes imaging polarimeters, will allow the evaluation of optical anisotropy response and diffraction characteristics of polarization hologram inscribed in the new series of azopolymers.

1.2 Problem Statement

Cylindrical vector beams (CVBs) show great potential in multiplexing information due to their mode orthogonality, but there is a lack of a CVB sorter for signal demultiplexing. Vector (or polarization) holography offers the means to storage and process optical information using polarized light. In this regard, synthesis, characterization and applications of photoanisotropic polymer films have been of interest for a long time due to the unique properties of the polarization holographic elements that can be implemented. Drawing on the capacity of specially synthesized side-chain azobenzene-containing polymers consisting in recording linear and circular birefringence, radially and azimuthally polarized beams are superimposed to obtain novel vector holographic diffraction gratings. This research project address the issue of analyzing, theoretically and experimentally, the spatial vector features of diffracted beams and evaluation of photoinduced anisotropies of the recorded vector gratings using Stokes and Mueller imaging polarimetry.

1.3 Objectives of the Study

The objectives pursued in this work are:

- Obtain the holographic process to record and reconstruct polarized light fields.
- Synthesize five photoreactive polymers and characterize their chemical structure.
- Characterize recording and performance of novel polarization diffractive elements using Stokes vector and Mueller matrix imaging polarimetry.
- Write, in collaboration with advisors, a scientific manuscript to be submitted for publication in a international peer-reviewed journal.

1.4 Research Questions

Diffraction features of polarization holographic gratings inscribed in thin films of azobenzene-containing polymers have attracted much interest for a long time. In this regard, the simultaneous surface relief shaping and photoinduced bulk anisotropy have been investigated with the aim of developing innovative applications for the generation and analysis of polarized light. Because of the above, this proposal is intended to contribute in this field evaluating the feasibility to record a new polarization diffractive element by holographic means: A vector vortex holographic grating. In order to predict its performance, a physics model considering the photoanisotropic response of azobenzene-containing polymers is developed and numerically evaluated. On this basis, when the vector vortex holographic grating is illuminated with a cylindrical vector light field used in the recording process it is expected that first-order diffraction beam reconstruct the orthogonal one.

1.5 Significance of the Study

An optical information channel usually carries multiplexed signals and demultiplexers are key to retrieve information. Most of the known structured light beam sorters are developed to identify orbital angular momentum states. Nonetheless, and beyond the scope of this thesis, cylindrical vector beam sorters with spin-dependent spiral transformation has been reported using liquid-crystal photoalignment technology and polarization-sensitive metasurfaces. Herein, this is the first time to our knowledge that feasibility of designing a holographic cylindrical vector beam sorter is proposed. At this stage, two orthogonal cylindrical vector beams will be used to inscribe a vector vortex grating in an azobenzene-containing polymer thin film, photoreactive material that is able to record full polarization patterns. Further research should be done in the future

to investigate the multiplexing capacity of the holographic photoreactive material and demultiplexing performance of the proposed diffractive element.

1.6 Structure of the Thesis

This writing is made up of 6 chapters, within the second a broad review of literature is presented, where as the first point a short introduction will be given that is more in-depth with this research, some fragments of previous research related to the topic will be revealed, highlighting what is most important and has the most influence on this work. Likewise, some definitions and key words will be shown for a good understanding of the project and what we want to achieve, as well as some of the properties that azopolymers have, such as their absorption spectrum and photoinduced birefringence; holographic polarization gratings and vector holograms. Within the third chapter, a theoretical analysis of the coherent superposition of two orthogonal fields will be carried out, from which the Stokes parameters will be derived. In the same way, the theoretical representation of the photoinduced hologram of these two superimposed vector optical fields will be presented. In addition, a series of experimental arrangements of the methods used will be presented, which in this case was Stokes polarimetry. The method used for the synthesis of the azopolymers used in the films and their deposition will also be disclosed.

In chapter four, is written the experimental methods, chapter five reports the results of the photoinduced birefringence curves of the azopolymers, in addition to the induction of spatial distributions of birefringence and the vector holograms. To conclude this writing, in chapter 6, the discussions and conclusions reached with this research work carried out in collaboration with CIQA will be reported.

Chapter 2

Literature Review

2.1 Introduction

Azobenzene groups can be incorporated into a polymer, either dispersed in a polymer matrix or chemically bonded to the polymer molecule, inducing new photochemical phenomena in the material due to the N=N double bond response, such as photoisomerization that occurs in azobenzene groups when irradiated with UV or visible light. This phenomenon has increased interest in the study of polymers modified with azobenzene-type compounds, known as azopolymers.[20]

The properties and potential applications of an azopolymer, whether main or side chain, can be controlled synthetically. This is because they depend largely on the type of substituent and spacer group present in the structure of the azobenzene molecule attached to the polymer chain. [21]

The diffraction characteristics of polarization holograms enrolled in polymers containing azobenzene compound have attracted a lot of interest for a long time and there are still several open questions about how to model their answer to vector optical fields. In addition, the simultaneous formation of superficial reliefs and the photoinduced anisotropy are investigated with the objective of developing innovative applications for the generation and analysis of polarized light. Due to the above, this proposal intends to contribute in this field developing a new polarization diffraction element.

There are several antecedents of the use of this type of polymers, in this part some of them will be discussed, which are considered the most important ones.

2.2 Body of the review

2.2.1 Research synthesis

Photochromic molecules are typically embedded in solid matrices for both fundamental and practical studies, which leads to photochromism being influenced by various matrix effects. In 2000, Kunihiro Ichimura did some research about Photoalignment of Liquid Crystal Systems; it says that the efficiencies of photochromism are influenced by various microenvironmental properties of the matrices, such as polarity, free volume, and interactions between molecules. Additionally, the structural changes in photochromic guest molecules can induce reversible alterations in the properties of the matrices, leading to reorientation of host molecules or residues within the matrices surrounding the guests. These matrix reorientations, triggered by photochromic molecules, enable the creation of versatile photofunctional materials and devices through photogenerated physical and chemical modifications of the matrices. [22, 23]

This type of effect, where photochromic molecules influence matrix properties, is characterized by significant molecular amplification. This occurs because the number of host molecules undergoing orientational transformations is much larger than the number of photochromic molecules acting as photoreceptors. Liquid crystals (LCs) naturally form supramolecular assemblies with unidirectional molecular orientations, resulting in optical anisotropy. [22] In this context, photoalignment of liquid crystals (LCs) refers to the control or manipulation of the orientational directions of LC molecules through photoirradiation. This is achieved by inducing optical anisotropy in photochromic layers or films. The optical anisotropy arises from the photoinduced molecular orientation of the photochromic units.[23]

The irradiation of a thin film of a polymer with azobenzene side chains with UV light results in the formation of a photostationary state containing the Z isomer as a major component, which is reversed to the E isomer under illumination with blue light.(Fig.2.1)

When the light is linearly polarized, photons are absorbed by azobenzene molecules according to $\cos^2\theta$, where θ is the angle between the electric dipole transition moment and the electric-field vector of the light used to undergo the photoselection leading to the molecular reorientation.

Liquid crystal copolymers with azobenzene side chains exhibit azimuthal reorientation of the chromophores, which in turn induces the reorientation of photoinactive mesogenic side chains.

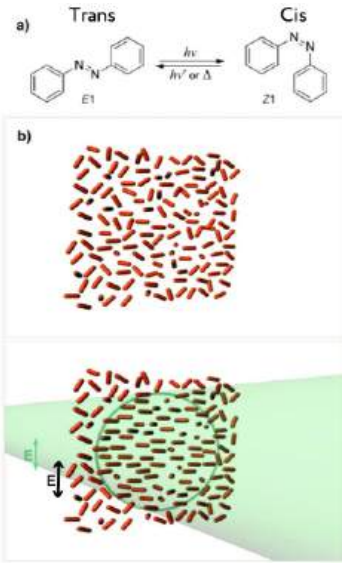

Figure 2.1: a) E–Z isomerization of azobenzene. b) Photoinduced alignment of azobenzene moieties (Weigert effect) [24]

The photochemical alteration of structures and orientations of a monolayered photochromic unit causes orientational changes throughout the LC (Liquid crystal) layer. [24]

2.2.2 Properties of Azopolymers: Absorption Spectra, Photoinduced Birefringence, Holographic Polarization Gratings, Vector Holograms

Diffraction gratings are optical devices used in scientific and technological fields. They consist of a series of finely spaced parallel lines or grooves etched onto a surface, which diffract light and split it into its component wavelengths.[25] This creates a spectrum, which can be defined as the visual representation of light separated into its individual wavelengths. In holography, this gratings are used to characterize holographic materials being the simplest hologram that can be recorded. A hologram is a three-dimensional image that uses the interference of light patterns to record and reconstruct information about an object, capturing both the intensity and phase of the light, which allows the object to be viewed in three dimensions from different angles. Therefore, a holographic diffraction grating is created by exposing a photosensitive material, like film or photopolymer, to the interference pattern generated by two laser beams. This interference pattern imprints a grating onto the material's surface, with the lines or grooves representing the diffraction characteristics of the light.[25]

The azobenzene is a photoswitchable compound, light irradiation can induce reversible *trans* to *cis* isomerization. This property enables the use of light to control a variety of properties of azobenzene containing materials, such as their polarity, solubility, melting points, glass transition temperature (Tg) values, viscosity, wrinkles, morphology, mechanical properties,etc. [10]

Hermann Rau divided azobenzenes into three types which can be seen in the Figure 2.2. The first one are azobenzene-type compounds bearing alkyl, aryl, halide, carbonyl, amide, nitrile, ester, and carboxylic acid substituents. The $\pi \rightarrow \pi^*$ and $n \rightarrow \pi^*$ absorption bands of *trans* azobenzene are located in the UV range and visible range, respectively. UV irradiation induces trans-to-cis isomerization. [10]

The second type are aminoazobenzene-type compounds having at least one amino or hydroxyl group located ortho or para to the azobenzene group. The $\pi \rightarrow \pi^*$ absorption band of the trans isomer is bathochromically shifted to 400–450 nm, partially overlapping with the $n \rightarrow \pi^*$ absorption band. The third type Rau described are pseudo-stilbene-type compounds containing a push–pull substitution to the azobenzene group. Their $\pi \rightarrow \pi^*$ absorption band and $n \rightarrow \pi^*$ absorption band are both located in the visible range, completely overlapping with each other. These types of azobenzene compounds have a fast rate for photoisomerization. [26, 10, 27]

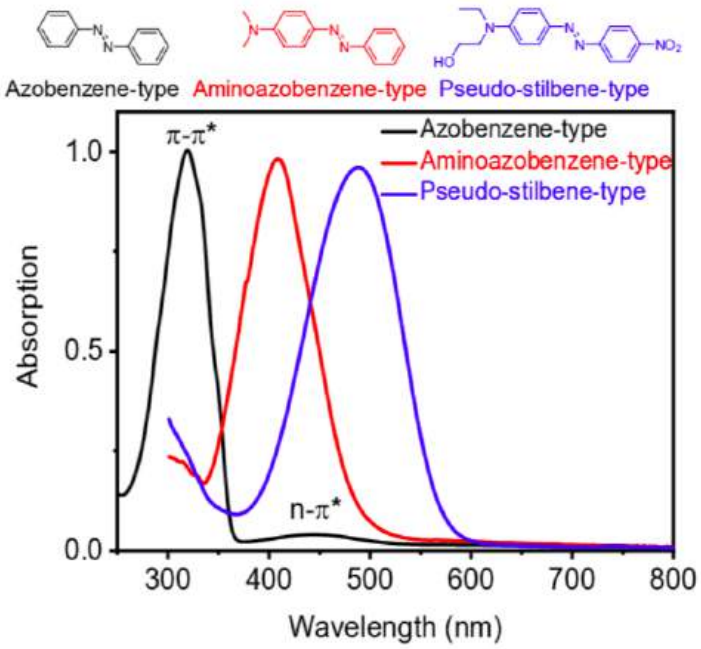

Figure 2.2: Chemical structures and UV/Vis absorption spectra of three types of azobenzenes. [10]

The trans-cis isomerization process is also often accompanied by a color change to

more intense shades. The absorption spectra of both isomers differ fundamentally in the following aspects: In the *trans* isomer the absorption band $\pi \rightarrow \pi^*$ is very intense, while $n \rightarrow \pi^*$ appears much weaker, because this transition in the trans isomer is not allowed by the symmetry rules. In the *cis* isomer the $\pi \rightarrow \pi^*$ band shifts to shorter wavelengths, decreasing markedly in intensity. On the other hand, the $n \rightarrow \pi^*$ electronic transition (380-520 nm) in the *cis* isomer is allowed, resulting in an increase in the intensity. [28]

Photoinduced anisotropy in side-chain azobenzene-containing polymer (SCACP) films is due to a mesogen molecular axis alignment after multiple trans-cis-trans isomerization cycles. Generally, this configurational isomerism occurs by absorption of proper wavelength laser irradiation and it is monitored reading with a laser probe having a wavelength far from the absorption bands. The alignment rate and saturation level depend, among other factors, on the spacer length and matrix rigidity. When SCACP films are excited with linearly polarized light, an effective linear birefringence can be obtained. A linearly polarized probe beam, with vibration plane subtending a 45° angle with the excitation vibration plane, is used to follow the alignment dynamics measuring the transmitted state of polarization.

Then, knowing the film thickness (d) , the instantenous birefringence $\Delta n(t)$ is given as

$$\Delta n(t) = \frac{\lambda}{2\pi d} \tan^{-1}\left(\frac{V_r(t)}{U_r(t)}\right) \tag{2.1}$$

where $U_r(t)$ and $V_r(t)$ are the third and fourth Stokes parameters measured for the reading laser beam, and λ_r is the reading wavelength. There are also another interesting photoinduced structures obtained when azopolymer films are irradiated with elliptically polarized light that depend on wavelength and ellipticity, which are classify as supramolecular chirality.[29]

Polarization holographic gratings are frequently used to characterized recording performance of SCACP films. These are induced by coherently superimposing two orthogonally homogeneously polarized beams with propagation vectors subtending a small angle. The resultant optical field is spatially modulated in state of polarization, and it is frequently referred as a vector optical field. For example, let us assume that left circularly polarized (LCP) field is superimposed to other right circularly polarized (RCP) field subtending an angle θ with propagation vectors contained in the xz-plane. The resultant field over the xy-plane can be described, using Stokes notation, by

$$\vec{S}(x) = \begin{bmatrix} 1 & \cos(2kx\sin\theta) & \sin(2kx\sin\theta) & 0 \end{bmatrix}^T \tag{2.2}$$

where $k = 2\pi/\lambda$ and superscript T is for the transpose. The above vector describe a linearly polarized (LP) field where the orientation is changing as a function of x , see case III in Fig.2.3.

These field induces a birefringent grating in the SCACP film. When the polarization hologram is reconstructed using LCP light beam, only one LCP diffraction order is obtained. On the other hand, when the polarization grating is illuminated with a LP light beam, two orders with opposite handedness are obtained.

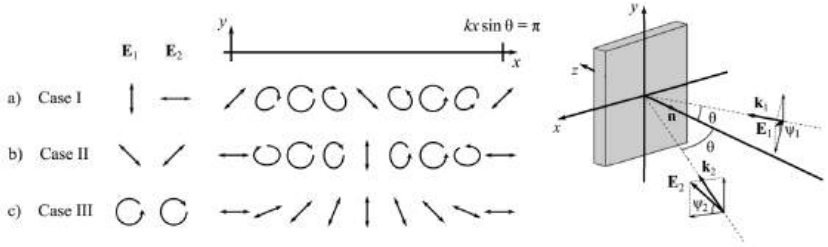

Figure 2.3: Spatially modulated polarization patterns obtained when superimposing two polarized beams with orthogonal states of polarization.[30]

Theory to study polarization patterns formed by superposition of ortogonal vector optical fields should be developed. Let us, however, introduce azimuthally and radially linearly polarized beams, which are given as

$$\vec{S}(\phi) = \begin{bmatrix} 1 & \cos(2\phi) & \pm\sin(2\phi) & 0 \end{bmatrix}^T \tag{2.3}$$

where

$$\phi = \tan^{-1}\left(\frac{y}{x}\right) \tag{2.4}$$

being x and y the Cartesian coordinates in the beam transversal plane. These optical vector fields will be superimposed subtending a small angle and using one of them as a reference polarized beam $R(x, y)$ in order to produce a complex spatial polarization modulation. This is,

$$\vec{H}(x, y) = \vec{S}(\phi) + \vec{R}(x, y). \tag{2.5}$$

With the aim of recording a novel polarization hologram, a SCACP film will be placed at the superposition plane. The polarized diffraction field produced by the photoinduced birefringent diffractive element will be analyzed by Stokes imaging polarimetry.

2.3 Previous Research

The article "Photoalignment of Liquid-Crystal Systems" by Kunihiro Ichimura (2000) is a comprehensive review on the light-induced control of the orientation of liquid crystal (LC) systems through photoactive molecules, mainly photochromic molecules such as azobenzenes. This study focuses on how light irradiation can induce molecular alignment changes in these systems, opening up possibilities for a wide range of technological applications.[31] The paper explains that photoactive molecules are typically embedded in solid matrices, and when irradiated with light, they undergo structural changes that affect the orientation of the host molecules (LCs) surrounding them. This enables control over optical anisotropy, which is crucial for practical applications in photofunctional materials and devices. This paper explains that photoactive molecules are typically embedded in solid matrices, and when irradiated with light, they undergo structural changes that affect the orientation of the host molecules (LCs) surrounding them. This enables control over optical anisotropy, which is crucial for practical applications in photofunctional materials and devices.[31] The author highlights how Liquid Crystal's doped with photoactive molecules can undergo significant reorientation when exposed to polarized light. These effects are utilized in data storage and optical switching, due to mesophase changes in response to light. This type of system can generate holographic diffraction patterns and other optical modulations. Then, there are a section called Photochromic Liquid-Crystalline Polymers, where he describes how liquid crystalline polymers with azobenzene side chains exhibit light-induced optical changes. These materials, when exposed to polarized light, can alter their birefringence and dichroism, allowing them to be used in the creation of holographic networks and other optical memory applications. The article also describes how surfaces treated with photoactive molecules, known as "command surfaces," can control the alignment of liquid crystal molecules. These changes are achieved through alternating irradiation with UV and visible light. Depending on the nature of the photoactive molecules, the LC molecules can align homeotropically (perpendicular) or planar (parallel) to the surface. The light-induced control of LC alignment has a lot of practical applications. The improvements in the ability to manipulate LC orientation using light have opened new opportunities for enhancing display performance. This development is used for optical memory and data storage, it has the ability to controllably and reversibly reorient LCs and is useful for developing light-based data storage devices. Another application is in Photonic Devices and Sensors where the optical properties of these materials can also be adjusted for applications in advanced photonic devices. [31]

The fundamental mechanism in these systems is the reversible photoisomerization of the photochromic molecules (especially azobenzene), which can switch between two stable configurations (E and Z isomers). This change induces reorientation in the liquid crystals, resulting in a controlled adjustment of their optical properties. Polymer films with azobenzenes are particularly efficient in this process due to their thermal stability and ability to form stable LC alignments. [31]

The article concludes by stating that the photoalignment of liquid crystals is a promising technology with a wide range of applications. Command surfaces and photoactive polymers allow for precise and durable control over LC alignment. Advances in the synthesis of new materials and the refinement of photoalignment techniques will continue to drive the development of more efficient and versatile optical devices. [31]

The article "Light-induced motions in azobenzene-containing polymers" by Cristina Cojocariu and Paul Rochon (2004), analyzes the light-induced optical phenomena in polymers containing azobenzene groups. Azobenzene is known for its ability to isomerize between *trans* and *cis* configurations upon exposure to UV or visible light (Fig.2.4, which generates conformational changes in polymers containing these groups, triggering molecular, nanoscale and micrometric motions.[32]

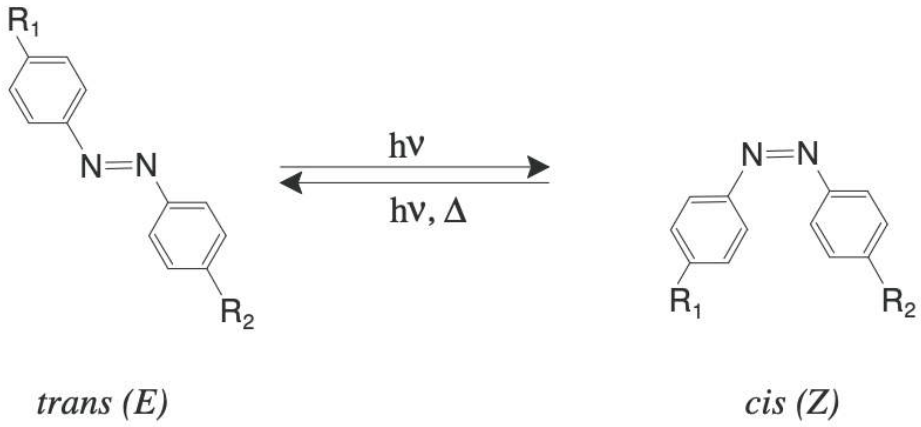

Figure 2.4: *Trans* and *cis* geometric isomers of azobence derivative.[32]

Polymers containing azobenzene chromophores have been studied mainly for their ability to induce *trans-cis-trans* photochemical isomerization, which can cause macroscopic variations in the chemical and physical properties of the materials. The rod-like structure of azobenzene also makes it well-suited for organization in liquid-crystalline (LC) mesophases. One of the most important properties of azobenzene chromophores is their ability to undergo photoisomerization, which leads to conformational changes in the polymer chains. The resulting effects include photo-orientation, birefringence,

surface relief grating (SRG) formation, and photoinduced chirality, with various potential applications in optical data storage, photonic devices, and more.[32]

There are three key levels at which light-induced motions occur in azobenzene-containing polymers.

- Molecular Level: The photoisomerization process causes individual chromophores to rotate and reorient when exposed to linearly polarized light (LPL). This leads to photo-orientation, a process where azobenzene chromophores align perpendicular to the light polarization, causing optical birefringence and dichroism in polymer films.

- Nanoscale Level: In organized environments, such as liquid crystals or crystalline domains, polarized light competes with the internal ordering forces. This results in the reorientation of entire domains, leading to large-scale motion within the nanometer range. This level of motion is more significant than that of individual chromophores.

- Micrometer Level: At this scale, the photoisomerization process results in large-scale material movement, leading to the formation of surface relief gratings (SRGs). These gratings are formed when a thin azopolymer film is exposed to an interference pattern of light, causing the polymer material to move across distances of micrometers. The exact mechanism behind SRG formation is still under investigation, but it is known to involve collective motion of the polymer chains.

Photoinduced birefringence refers to the creation of optical anisotropy in azopolymer films when exposed to polarized light. This effect was initially observed in liquid-crystalline polymers, but it has since been demonstrated in amorphous polymers as well. The ability to store optical information in these films has been widely studied, and the birefringence can be erased using circularly polarized light (CPL). This has implications for reversible optical storage.[32]

Several factors influence the extent of birefringence:

- Structural Factors: The size and shape of the azobenzene chromophores, as well as the flexibility of the polymer backbone, play a critical role. For instance, bulky chromophores hinder the motion necessary for birefringence, while polymers with longer spacers exhibit greater chromophore mobility.

- External Parameters: Temperature, light intensity, and film thickness all affect the dynamics of birefringence. For example, increasing temperature can cause the chromophores to lose their alignment, while higher light intensity can accelerate the orientation process.

One of the most exciting discoveries in azopolymer research is the formation of surface relief gratings (SRGs), which are sinusoidal patterns created on the surface of the polymer through mass transport triggered by light. These gratings can reach depths of several micrometers and have important technological applications in holography, waveguides, and optical filters.

SRGs are produced when azopolymer films are exposed to interference patterns of coherent light. Over time, the chromophores undergo photoisomerization cycles that result in the movement of the polymer material. The driving force behind this movement is still under study, but researchers believed to be linked to the internal stresses caused by the repeated isomerization cycles. [32]

The depth and quality of SRGs can be controlled by adjusting the polarization state of the light, exposure time, and angle of inscription. High diffraction efficiency can be achieved, and the gratings are highly stable at room temperature.

In liquid-crystalline azopolymers, photoinduced birefringence is amplified due to cooperative motion. When some azobenzene groups undergo motion, they cause neighboring groups to follow suit, resulting in large-scale organization. This amplification effect is most pronounced in liquid-crystalline systems but can also be observed in amorphous polymers. A fascinating effect of azobenzene is the ability to induce chirality in otherwise achiral polymer films through exposure to circularly polarized light (CPL). This results in the formation of helical supramolecular structures, whose handedness depends on the polarization direction of the light. This phenomenon can be reversed by switching the handedness of the CPL, making it a candidate for chiroptical switching applications. [32] The induced chirality can be erased and rewritten repeatedly by alternating the polarization of the light source. Azobenzene polymers exhibit photorefractive properties, which make them suitable for applications such as holographic data storage. Photorefractivity in azopolymers arises from a combination of nonlinear optical properties and photoconductivity. These materials can potentially combine birefringence, surface relief formation, and photorefractivity, making them promising for the development of all-optical devices. This paper highlights the transformative potential of azobenzene polymers in creating all-optical devices, holographic storage

systems, and even chiral materials, making them a versatile tool in modern material science and photonics. [32]

The document "Fotoisomerización de azobencenos: movimientos moleculares a la carta", written by María Ribagorda and Estibaliz Merinob provides a comprehensive study of azobenzenes, a class of organic compounds with significant importance in modern chemistry due to their reversible photoisomerization between cis and trans forms. This reversible process triggers molecular movements and spatial geometry changes, making azobenzenes excellent candidates for the development of molecular devices, such as switches and nanomachines.[28] Azobenzenes are composed of two aromatic groups connected by an azo (-$N = N$-) bond. Their photochemical and thermal isomerization properties allow the transformation between two geometric forms: the more stable trans isomer and the less stable cis isomer. Upon exposure to light, a significant transformation in their physical properties, such as molecular geometry, dipole moment, and absorption spectrum, takes place. This change has driven the development of azobenzene-based systems as dynamic molecular devices.[28]

For the isomerization process, the *trans* isomer is almost planar and has a dipole moment close to zero, while the *cis* isomer adopts an angular geometry, with a dipole moment of approximately 3 D. When the azobenzene chromophore is exposed to UV light, it undergoes a *trans*-to-*cis* isomerization, which reduces the distance between the most distant positions of the aromatic rings from 9.0 Å to 5.5 Å. This photoisomerization significantly alters the molecule's spatial conformation, which can be used to modulate a variety of molecular behaviors.[28]

Azobenzenes meet several important requirements to function as molecular switches, some of them are:

- Reversible interconversion between two species by irradiation with light of a certain wavelength.
- Thermal stability, allowing the storage of information.
- High fatigue resistance, enabling multiple cycles without degradation.
- Fast response times and high quantum yields for efficient switching.

Azobenzenes are one of the most versatile systems in molecular photochemistry, offering potential for the development of molecular devices, including switches, sensors, and motors. The reversible isomerization process allows for the precise control of molecular conformation and movement, which can be applied in numerous fields, from biology to nanotechnology. The ongoing research aims to improve the properties of

azobenzene systems and expand their applications in advanced photomechanical and biochemical systems.[28]

In the article entitled "Cyano azobenzene polymer films: Photo-induced reorientation and birefringence behaviors with linear and circular polarized light", the authors study the behaviors of cyano-azobenzene polymer films. The polymer films are made from polymethacrylate with cyano azobenzene side groups. The study highlights that illumination of these films with polarized and unpolarized light leads to a color change, making the film darker, which contrasts with typical azo polymers that tend to bleach under light. The photoisomerization process is examined, revealing that the color change is not due to interactions between dye molecules. Time-resolved experiments show rapid changes in isomer populations under high light power. [33] Notably, experiments on light-induced birefringence (LIB) demonstrate exceptional stability, with circular polarized light not erasing birefringence but actually inducing anisotropy, suggesting a phase transition in the polymer. Azo dyes are widely used in various applications due to their ability to undergo photoisomerization, leading to changes in molecular shape and optical properties. The document elaborates on the photoresponsive properties of azobenzenes, specifically the reorientation of chromophores under polarized light. The study focuses on cyanoazobenzene as an effective compound for creating devices with anisotropic molecular order. The polymer studied is a methacrylate compound synthesized by Stanislaw Kucharski, containing cyanoazobenzene as a side group. The characterization methods that were employed to analyzed absorption and transmission were spectroscopy techniques, as well as to evaluate the effects of different light sources of the polymer. For the birefringence measurement, a set up with crossed polarizers and a pump beam was used.[33]

The absorption spectra shifts with illumination, indicating a phase transition. Both polarized and unpolarized light induce molecular reorientation. The time evolution of absorbed light shows that higher pump intensities lead to faster changes in isomer populations. The polymer exhibits significant birefringence when is exposed to linear polarized light. The birefringence does not relax when light is turned off, suggesting a lasting phase transition. Circular polarized light in this polymer induces birefringence, further supporting the idea of a photo-induced phase transition. The cyano-azobenzene polymer films demonstrate unique properties, such as as stable birefringence under circular polarized light and efficient photoisomerization. The findings reveal that these materials can be suitable for advanced optical applications due to their large nonlinearity and potential for inducing anisotropic states. [33]

The article "Photoinduced birefringence of azobenzene polymer at blue excitation wavelenghts" authored by Anna Kozanecka-Szmigiel, Krzysztof Switkowski, Ewa Schab-Balcerzak, and Dariusz Szmigiel investigates the photoinduced birefringence in azobenzene-functionalized poly(esterimide) (PEI) films under various blue excitation wavelengths (388, 420, and 438 nm).[34] Azobenzene polymers exhibit photoresponsive behavior due to the presence of azobenzene molecules, which can switch between two isomeric forms (trans and cis) in response to light. This switching induces optical anisotropy, leading to birefringence, which has potential applications in data storage, optical switching, and photomechanics. This study measured the birefringence induced by trans–cis–trans isomerizations at three excitation wavelengths. Significant differences in saturation levels and growth dynamics of birefringence were observed between the different wavelengths.[34] The 388 nm excitation (on the blue side of the absorption band) generated a larger final birefringence compared to the 420 nm and 438 nm excitations, nearly doubling the birefringence induced at these longer wavelengths. The growth of birefringence is influenced by the absorption characteristics of the cis isomer and the photoisomerization pathways. The results suggest distinct isomerization pathways for the cis isomers depending on the excitation wavelength. [34] The research involved synthesizing and characterizing the PEI polymer, followed by measuring the induced birefringence using a laser setup that provided controlled excitation at specified wavelengths. A Dektak XT stylus profiler was used to measure film thickness, and a UV-Vis spectrophotometer was employed to analyze the absorption characteristics. Birefringence growth was described by a biexponential equation, reflecting different reorientation processes of the azobenzene groups and polymer segments. The biexponential fit parameters indicated that the fastest process was influenced by the excitation wavelength, with notable differences observed in the amplitudes and time constants. The study concluded that excitation on the blue side of the absorption band resulted in greater birefringence but with slower dynamics compared to red-side excitation. The findings enhance the understanding of how excitation wavelength affects the photoinduced birefringence in azobenzene polymers, potentially informing future applications in photonics and materials science.[34]

Photoresponsive polymers, particularly those containing azobenzene groups, have garnered significant interest due to their ability to undergo reversible trans-cis photoisomerization when exposed to light. This property allows for the modulation of various physical properties such as polarity, solubility, melting points, and mechanical characteristics. Most existing studies focus on mono-azopolymers, which are those that contain a single azobenzene group per repeat unit. [10] However, recent advancements

as the ones described by T. Aida [35] have led to the development of multi-azopolymers, which incorporate multiple azobenzene groups, enhancing their photoresponsive capabilities.

The exploration of multi-azopolymers, which contain multiple azobenzene groups per repeat unit, presents new opportunities for enhancing photoresponsive properties. These polymers can be synthesized through various strategies like Covalent Incorporation, where azobenzene groups can be integrated into the polymer backbone or side chains, both in series and parallel configurations; and non-covalent methods where supramolecular chemistry allows for the introduction of azobenzene groups via hydrogen bonding, host-guest interactions, or ionic interactions, facilitating easier processing and improved solubility.[10]

The author reported the existence of three different types of multi-azopolymers:

- Non-Conjugated multi-Azopolymers: These involve azobenzene groups linked by flexible, non-conjugated linkers and can show enhanced alignment and order under processing conditions.
- Conjugated Multi-Azopolymers: Azobenzene groups connected via conjugated linkers can exhibit larger birefringence and stability in photoinduced states.
- Supramolecular Multi-Azopolymers: These polymers leverage non-covalent interactions for the incorporation of azobenzene units, showing promising solubility and processing benefits.

The unique characteristics of multi-azopolymers suggest numerous applications across various fields, including Optical Data Storage due to their ability to form surface relief gratings (SRGs) and exhibit high birefringence, reworkable adhesives, utilizing the reversible transitions of azobenzene moieties, and optoelectronic devices, multi-azopolymers can function as photoresponsive semiconductors with enhanced fatigue resistance.[10] The field of photoresponsive multi-azopolymers holds immense potential for innovation in material science and engineering. While significant progress has been made, further exploration of their properties, applications, and synthesis methods is essential to unlock their full capabilities and address existing challenges.

"Compact and scalable large vortex array generation using Azocarbazole Polymer and digital hologram printing technique" by Boaz Jessie Jackin, Masaki Shirai, Honoka Haginaka, Kenji Kinashi, Naoto Tsutsumi and Wataru Sakai. This research discusses a method for generating a large number of multiplexed optical vortex beams which are essential for advancing information photonics. This paper aims to develop an

integrated device to generating a large array of optical vortex beams with an arbitrary topological charges, addressing the need for compact and scalable systems in photonics. [36]The researchers employed a combination of computer-generated holography, digital hologram printing and photoisomeric polymers. The polymer film used is 1 mm^2 in size and 30 μm thick, demonstrating the capability to generate 100 multiplexed optical vortex beams. The polymer film exhibited diffraction efficiency of 30% and maintained its properties for over 50 days. The technique allows the emission of a predetermined vortex array when illuminated with a collimated laser beam. A 10×10 optical vortex array with a topological charge of $l = 10$ was successfully generated. The authors discuss the limitations of existing vortex beam generation methods, highlighting that most approaches are bulky and not scalable. The proposed method overcomes these challenges by utilizing integrated optics, which scales linearly with performance rather than exponentially. The generated optical vortex arrays are viewed as beneficial for information processing, as each vortex beam can interact independently with other media. This capability makes them useful for advanced tasks in optical computing and communication.[36] The research suggests that further advancements could include increasing the array size and topological charges through techniques such as hologram stitching. The authors also mention the potential for dynamic generation of vortex arrays, which remains a challenge but is essential for real-time applications. The authors conclude that their technique for generating optical vortex arrays is compact, scalable, and holds promise for integration into optical computing and communication technologies.[36]

Chapter 3

Theoretical framework

3.1 Introduction

Spatial modulation of the state of polarization in its transverse section is one of the distinctive features of optical vector beams (OVBs). Polarization or vector holography is about the recording of polarization patterns resulting from the coherent superposition of two mutually coherent monochromatic beams, usually with orthogonal states of polarization, in a photoresponsive material. The simplest polarization holograms are birefringent and/or diattenuant gratings with unique reconstruction properties.

3.2 Polarized light

Light is an electromagnetic wave (EMW) that is fully describe by a set of three orthogonal vectors (thriad) related to the electric (**E**) and magnetic (**B**) field amplitudes, as well as the propagation direction (**k**).[37] Usually, it is enough to consider **E** for the EMW propagation analysis through a lossless dielectric medium. In order to define the state of polarization of a light beam, which implies the vector nature of light, it is necessary to assume that it is a plane monochromatic wave.[38] Besides, further simplification requires that the propagation vector **k** be parallel to the $z-$axis. In this manner, a vector equation to represent the EMW is given as

$$\mathbf{E}(z,t) = E_{0x}\cos\left(kz - \omega t + \phi_x\right)\hat{\mathbf{i}} + E_{0y}\cos\left(kz - \omega t + \phi_y\right)\hat{\mathbf{j}}, \tag{3.1}$$

where E_{0x} and E_{0y} are the electric field components along the $x-$ and $y-$axis, respectively. $k = |\mathbf{k}|$ is the wavenumber, ω is the angular frequency of the oscillating field, and ϕ_x and ϕ_y are the absolute phases of $x-$ and $y-$axis components, respectively. [37] Light wavelength is the oscillation spatial period of the wave that is defined as $\lambda = 2\pi/k$. Light frequency is the oscillation time period of the wave that is given as

$f = \omega/(2\pi)$. A more convenient notation to represent an EMW is based in complex functions, namely,

$$\begin{aligned}\mathbf{E}(z,t) &= E_{0x}e^{i(kz-\omega t+\phi_x)}\hat{\mathbf{i}} + E_{0y}e^{i(kz-\omega t+\phi_y)}\hat{\mathbf{j}}, \\ &= e^{i(kz+\phi_x)}\left(\tilde{E}_{0x}\hat{\mathbf{i}} + \tilde{E}_{0y}e^{i\Delta\phi}\hat{\mathbf{j}}\right),\end{aligned} \tag{3.2}$$

where $\tilde{E}_{0x} = E_{0x}e^{-i\omega t}$ and $\tilde{E}_{0y} = E_{0y}e^{-i\omega t}$ are complex amplitudes of $x-$ and $y-$ phasor components, respectively. $\Delta\phi = \phi_y - \phi_x$ is the relative phase between orthogonal electric field components.[38] Taking the real part of Eq. (3.2) results in an equivalent expression to Eq. (3.1).

The state of polarization of a light beam can be defined using Eq. (3.2). Let us consider that an observer located at $z = 0$ can see the figure, a closed conical section, traced by the end of the resultant electric field vector over the $xy-$plane as time goes by.[37] Assuming that $\phi_x = 0$, there are some particular cases:

- If $\Delta\phi = n\pi$, where n is an even number, light is linearly polarized and oriented at $\theta = +\arctan\left(|\tilde{E}_{0y}|/|\tilde{E}_{0x}|\right)$ with respect the $x-$axis. On the other hand, if $\Delta\phi = m\pi$, where m is an odd number, light is linearly polarized and oriented at $\theta = -\arctan\left(|\tilde{E}_{0y}|/|\tilde{E}_{0x}|\right)$ with respect the $x-$axis.

- If $|\tilde{E}_{0x}| = |\tilde{E}_{0y}|$ and $\Delta\phi = (2n+1)\pi/2$, where n is an even number, light is circularly polarized with left handedness (counter-clockwise rotation). However, if $|\tilde{E}_{0x}| = |\tilde{E}_{0y}|$ and $\Delta\phi = (2m+1)\pi/2$, where m is an odd number, light is circularly polarized with right handedness (clockwise rotation).

Any other setting values of the light beam parameters will represent an elliptical state of polarization with handedness to be determined.[38]

3.2.1 Jones vector notation

Polarized light can be represented using a normalized column matrix of the order 2×1, also known as Jones vector. The first row is the $x-$component of the electric field $\mathbf{E}(z,t)$ given in Eq. (3.2), while the second row corresponds to the $y-$component. Considering that state of polarization is defined at $z = 0$ and that time oscillations are the same for field components, both dependencies can be discarded.[39] In this manner, the polarized light beam can be written as

$$\mathbf{E} = \frac{1}{\sqrt{E_{0x}^2 + E_{0y}^2}}\begin{pmatrix} E_{0x} \\ E_{0y}e^{i\Delta\phi}\end{pmatrix}, \tag{3.3}$$

where it has been also omitted the reference phase of $x-$component $e^{i\phi_x}$. Using the special cases defined above, the typical Jones vectors, shown in Table 3.1, are obtained.

Table 3.1: Jones vectors for polarized light with typical states.

State of polarization	Jones vector
Horizontal linearly polarized	$\begin{pmatrix} 1 \\ 0 \end{pmatrix}$
Vertical linearly polarized	$\begin{pmatrix} 0 \\ 1 \end{pmatrix}$
θ-oriented linearly polarized	$\begin{pmatrix} \cos\theta \\ \sin\theta \end{pmatrix}$
Right circularly polarized	$\frac{1}{\sqrt{2}}\begin{pmatrix} 1 \\ -i \end{pmatrix}$
Left circularly polarized	$\frac{1}{\sqrt{2}}\begin{pmatrix} 1 \\ i \end{pmatrix}$

Light with elliptical state of polarization with the major semiaxis oriented horizontally is represented with the following Jones vector,

$$\mathbf{E} = \begin{pmatrix} \cos\varepsilon \\ i\sin\varepsilon \end{pmatrix}, \tag{3.4}$$

where $\tan\varepsilon = E_{0y}/E_{0x}$ being ε the ellipticity angle, $|\varepsilon| \leq \pi/2$. Handedness of elliptically polarized light is given by ε sign. Furthermore, when the major semiaxis is oriented at an angle θ, the Jones vector in Eq. (3.4) is transformed to

$$\mathbf{E} = \begin{pmatrix} \cos\theta\cos\varepsilon - i\sin\theta\sin\varepsilon \\ \sin\theta\cos\varepsilon + i\cos\theta\sin\varepsilon \end{pmatrix}. \tag{3.5}$$

From this last expression, the solution for the inverse problem can be found. Namely, unknown ellipticity and major semiaxis orientation angles of an arbitrary Jones vector can be retrieved using

$$\tan 2\theta = \frac{2\mathrm{Re}\{\chi\}}{1-|\chi|^2}, \tag{3.6}$$

$$\sin 2\varepsilon = \frac{2\mathrm{Im}\{\chi\}}{1+|\chi|^2}, \tag{3.7}$$

where χ is a complex number defined as

$$\chi = \frac{E_{0y}}{E_{0x}} e^{i\Delta\phi}. \tag{3.8}$$

In Eq. (3.5), a rotation transformation has been applied to the Eq. (3.4). This can be achieved by matrix product operation expressed as

$$\mathbf{E}(-\theta) = \mathbf{R}(-\theta)\,\mathbf{E}(0), \tag{3.9}$$

where

$$\mathbf{R}(\theta) = \begin{pmatrix} \cos\theta & \sin\theta \\ -\sin\theta & \cos\theta \end{pmatrix}, \tag{3.10}$$

is known as the rotation matrix.

3.2.2 Stokes vector notation

In the experimental research is practical to represent polarized light using Stokes vector notation instead of the Jones vector one. Stokes vector is a 4×1 column matrix of real numbers, each representing measured intensity values.[37] This is defined as

$$\mathbf{I} = \begin{pmatrix} I \\ Q \\ U \\ V \end{pmatrix} = \begin{pmatrix} \langle E_x^* E_x \rangle + \langle E_y^* E_y \rangle \\ \langle E_x^* E_x \rangle - \langle E_y^* E_y \rangle \\ \langle E_x^* E_y \rangle + \langle E_y^* E_x \rangle \\ -i\left[\langle E_x^* E_y \rangle - \langle E_y^* E_x \rangle\right] \end{pmatrix} = \begin{pmatrix} I_x + I_y \\ I_x - I_y \\ I_{+\pi/4} - I_{-\pi/4} \\ I_R - I_L \end{pmatrix}, \tag{3.11}$$

where I (or S_0), Q (or S_1), U (or S_2) and V (or S_3) are identified as the first, second, third and fourth Stokes parameters, respectively. Angle brackets, $\langle\cdot\rangle$, represent time average of auto- or cross-correlation of electric field components E_x and E_y.[37] This representation is useful when coherence properties of the source affect state of polarization of emitted light. I_x and I_y are intensities measured along the $x-$ and $y-$axis, $I_{+\pi/4}$ and $I_{-\pi/4}$ are intensities measured along $\pm\pi/4$ angles, and I_R and I_L are intensities of right and left circularly polarized light. Then, the determination of Stokes parameters of an arbitrary light beam requires six intensities measurements.[38] Nonetheless, when the analyzed beam is fully polarized and propagates through lossless optical polarizing analyzers, only four measurements are needed and

$$\mathbf{I} = \begin{pmatrix} I \\ 2I_x - I \\ 2I_{+\pi/4} - I \\ 2I_R - I \end{pmatrix}, \tag{3.12}$$

where $I = I_x + I_y = I_{+\pi/4} + I_{-\pi/4} = I_R + I_L$.

An arbitrary Stokes vector with ellipticity angle ε and major semiaxis orientation θ can be represented numerically using

$$\mathbf{I} = I \begin{pmatrix} 1 \\ \cos 2\varepsilon \cos 2\theta \\ \cos 2\varepsilon \sin 2\theta \\ \sin 2\varepsilon \end{pmatrix}. \tag{3.13}$$

Then, ε and θ can be retrieved from experimental measurements through

$$\theta = \frac{1}{2}\tan^{-1}\left(\frac{U}{Q}\right), \tag{3.14}$$

$$\varepsilon = \frac{1}{2}\sin^{-1}\left(\frac{V}{I}\right). \tag{3.15}$$

Typical full polarized light beams, like those presented for Jones notation, are presented in Table 3.2. Stokes notation allows to represent partially polarized or unpolarized light, where cross-correlation between orthogonal electric field components is affected by random fluctuations.[37] In this regard, the parameter referred as degree of polarization DoP is defined as

$$DoP = \frac{\sqrt{Q^2 + U^2 + V^2}}{I}, \quad 0 \leq DoP \leq 1. \tag{3.16}$$

Then, Eq. (3.13) is rewritten for partially polarized light as

$$\mathbf{I} = I(1 - DoP)\begin{pmatrix}1\\0\\0\\0\end{pmatrix} + I\ DoP\begin{pmatrix}1\\\cos 2\varepsilon\cos 2\theta\\\cos 2\varepsilon\sin 2\theta\\\sin 2\varepsilon\end{pmatrix}. \tag{3.17}$$

Stokes vector in the first term on the right-hand side of Eq. (3.17) is the representation of unpolarized light.

3.3 Optical anisotropy in matter

When a polarized beam of light propagates through an anisotropic medium, it experiences a linear transformation. The first anisotropic property of matter to be discussed herein is diattenuation, formerly known as dichroism.[37] A pure diattenuator is a medium that absorbs light orthogonal vector components differently. On the other hand, in a pure birefringent medium, vector components of the electromagnetic wave propagates through at different speeds. The last property is depolarization. A depolarizing medium breaks the phase correlation between the orthogonal components of the electric field, thus, reducing the degree of polarization.[37] In general, these properties are not always completely isolated and the joint effect is observed.[39]

3.3.1 Jones matrix notation

The linear transformation induced by an anisotropic medium in a polarized light beam propagating through can be represented by a 2×2 matrix with complex coefficients,

$$\mathbf{J} = \begin{pmatrix}J_{11} & J_{12}\\J_{21} & J_{22}\end{pmatrix}, \tag{3.18}$$

Table 3.2: Stokes vectors for polarized light with typical states.

State of polarization	Stokes vector
Horizontal linearly polarized	$\begin{pmatrix} 1 \\ 1 \\ 0 \\ 0 \end{pmatrix}$
Vertical linearly polarized	$\begin{pmatrix} 1 \\ -1 \\ 0 \\ 0 \end{pmatrix}$
θ-oriented linearly polarized	$\begin{pmatrix} 1 \\ \cos 2\theta \\ \sin 2\theta \\ 0 \end{pmatrix}$
Right circularly polarized	$\frac{1}{\sqrt{2}} \begin{pmatrix} 1 \\ 0 \\ 0 \\ 1 \end{pmatrix}$
Left circularly polarized	$\frac{1}{\sqrt{2}} \begin{pmatrix} 1 \\ 0 \\ 0 \\ -1 \end{pmatrix}$

which is known as Jones matrix. One of these transformation is known as diattenuation, formerly known as dichroism, that is the difference in optical absorption between two orthogonal polarization components of a light beam.[39] In this regard, a linear diattenuator absorbs horizontal and vertical components of incident polarized light in a different rate and each following Beer-Lambert Law.[38] The Jones vector to represent this transformation is written as

$$\mathbf{J}_D = \begin{pmatrix} e^{-\kappa_x t} & 0 \\ 0 & e^{-\kappa_y t} \end{pmatrix}, \tag{3.19}$$

where κ_x and κ_y are the absorption coefficients of linear polarization intensity components along $x-$ and $y-$ axis, respectively, and t is the medium thickness.[39] Circular diattenuation is analog to the above definition, but the polarized field is represented in a circular polarization basis. Thus, a circular diattenuator absorbs different right and left circularly polarized light.[38] Another frequent transformation is retardation that is based in birefringence, namely, the existence of a different refractive index for each orthogonal polarization component of a light beam.[39] A linear retarder transforms an

incident polarized beam by the matrix operator given as

$$\mathbf{J}_R = \begin{pmatrix} e^{ikn_x t} & 0 \\ 0 & e^{ikn_y t} \end{pmatrix}, \tag{3.20}$$

where n_x and n_y are the refractive indices experienced by $x-$ and $y-$intensity components of incident polarized light, respectively, and $k = 2\pi/\lambda$ is the wavenumber.[38] Circular retarder also introduces a phase difference between orthogonal components of the polarized light, but in this case the representation is in the circular polarization basis. In Table 3.3, Jones matrices for some typical idealized polarizing elements are presented. However, when an optical sample is characterized, it is found that two or more of this transformations are present.

Table 3.3: Idealized Jones matrices for typical polarizing optical elements. T is the transmittance, a dimensionless number defined by the ratio of the radiant flux transmitted to the incident radiant flux.

Polarizing element	Jones matrix
Neutral density filter	$T\begin{pmatrix} 1 & 0 \\ 0 & 1 \end{pmatrix}$
Linear polarizer with transmission axis at 0	$\begin{pmatrix} 1 & 0 \\ 0 & 0 \end{pmatrix}$
Linear polarizer with transmission axis at $\pi/2$	$\begin{pmatrix} 0 & 0 \\ 0 & 1 \end{pmatrix}$
$\lambda/4$-retardation plate with fast axis at 0 and $\pi/2$	$\begin{pmatrix} 1 & 0 \\ 0 & \pm i \end{pmatrix}$
$\lambda/2$-retardation plate with fast axis at 0 or $\pi/2$	$\begin{pmatrix} 1 & 0 \\ 0 & -1 \end{pmatrix}$
$\pi/2$-Optical rotator	$\begin{pmatrix} 0 & -1 \\ 1 & 0 \end{pmatrix}$
Right and left circular polarizer	$\frac{1}{2}\begin{pmatrix} 1 & \pm i \\ \pm i & 1 \end{pmatrix}$

On the other hand, the total transformation effect of a system of N-polarizing elements on an incident polarized beam can be represented as

$$\mathbf{J}_T = \mathbf{J}_N\, \mathbf{J}_{N-1}\, \ldots\, \mathbf{J}_2\, \mathbf{J}_1, \tag{3.21}$$

where the first element at the system input is $\mathbf{J}_1$ and the last, at the system output, is $\mathbf{J}_N$. Sometimes is needed to represent an optical polarizing component in a rotated coordinate system.[37] The required matrix operation to find the new representation is

$$\mathbf{J}(-\theta) = \mathbf{R}(-\theta)\mathbf{J}(0)\mathbf{R}(\theta), \tag{3.22}$$

where $\mathbf{R}(\theta)$ is the rotation matrix, Eq. (3.10).

3.3.2 Mueller matrix notation

In order to represent mathematically the linear transformation induced by an anisotropic medium in a polarized beam given in the Stokes vector notation, a Mueller matrix is introduced that is a 4×4 array of real numbers given as

$$\mathbf{M} = \begin{pmatrix} m_{11} & m_{12} & m_{13} & m_{14} \\ m_{21} & m_{22} & m_{23} & m_{24} \\ m_{31} & m_{32} & m_{33} & m_{34} \\ m_{41} & m_{42} & m_{43} & m_{44} \end{pmatrix}. \tag{3.23}$$

In Table 3.4, Mueller matrices for idealized typical polarizing elements are presented.

Table 3.4: Idealized Mueller matrices for typical polarizing optical elements. T is the transmittance that is defined as above.

Polarizing element	Mueller matrix
Neutral density filter	$T \begin{pmatrix} 1 & 0 & 0 & 0 \\ 0 & 1 & 0 & 0 \\ 0 & 0 & 1 & 0 \\ 0 & 0 & 0 & 1 \end{pmatrix}$
Linear polarizer with transmission axis at 0	$\frac{1}{2} \begin{pmatrix} 1 & 1 & 0 & 0 \\ 1 & 1 & 0 & 0 \\ 0 & 0 & 0 & 0 \\ 0 & 0 & 0 & 0 \end{pmatrix}$
$\lambda/4$-retardation plate with fast axis at 0	$\begin{pmatrix} 1 & 0 & 0 & 0 \\ 0 & 1 & 0 & 0 \\ 0 & 0 & 0 & -1 \\ 0 & 0 & 1 & 0 \end{pmatrix}$
$\lambda/2$-retardation plate with fast axis at 0 or $\pi/2$	$\begin{pmatrix} 1 & 0 & 0 & 0 \\ 0 & 1 & 0 & 0 \\ 0 & 0 & -1 & 0 \\ 0 & 0 & 0 & -1 \end{pmatrix}$
$\pi/2$-Optical rotator	$\begin{pmatrix} 1 & 0 & 0 & 0 \\ 0 & -1 & 0 & 0 \\ 0 & 0 & -1 & 0 \\ 0 & 0 & 0 & 1 \end{pmatrix}$
Right and left circular polarizer	$\frac{1}{2} \begin{pmatrix} 1 & 0 & 0 & \pm 1 \\ 0 & 0 & 0 & 0 \\ 0 & 0 & 0 & 0 \\ \pm 1 & 0 & 0 & 1 \end{pmatrix}$

An arbitrary diattenuator having amplitude transmission coefficients p_x and p_y along

$x-$ and $y-$ axis, respectively, transforms an incident beam through the matrix

$$\mathbf{M}_D = \frac{1}{2}\begin{pmatrix} p_x^2+p_y^2 & p_x^2-p_y^2 & 0 & 0 \\ p_x^2-p_y^2 & p_x^2+p_y^2 & 0 & 0 \\ 0 & 0 & 2p_xp_y & 0 \\ 0 & 0 & 0 & 2p_xp_y \end{pmatrix}. \tag{3.24}$$

On the other hand, the Mueller matrix of a waveplate introducing a phase shift φ between orthogonal components of the electric field is written as

$$\mathbf{M}_W = \frac{1}{2}\begin{pmatrix} 1 & 0 & 0 & 0 \\ 0 & 1 & 0 & 0 \\ 0 & 0 & \cos(\varphi) & -\sin(\varphi) \\ 0 & 0 & \sin(\varphi) & \cos(\varphi) \end{pmatrix}. \tag{3.25}$$

Propagation properties through a set of polarizing components are similar to those described for the Jones matrices. Thus,

$$\mathbf{M}_T = \mathbf{M}_N\ \mathbf{M}_{N-1}\ \ldots\ \mathbf{M}_2\ \mathbf{M}_1, \tag{3.26}$$

where $\mathbf{M}_1$ and $\mathbf{M}_N$ are the first and last elements, respectively. Regarding the representation of a polarizing element in a rotated coordinate framework, this can be accomplished through the transformation given as

$$\mathbf{M}' = \mathbf{R}(-\theta)\ \mathbf{M}\ \mathbf{R}(\theta), \tag{3.27}$$

where

$$\mathbf{R}(\theta) = \begin{pmatrix} 1 & 0 & 0 & 0 \\ 0 & \cos(2\theta) & \sin(2\theta) & 0 \\ 0 & -\sin(2\theta) & \cos(2\theta) & 0 \\ 0 & 0 & 0 & 1 \end{pmatrix}. \tag{3.28}$$

3.4 Cylindrical vector beams

Recently, the generation and applications of light beams with spatial modulation of the polarization state over their cross section has generated much interest among researchers around the world.[40] Among the structured vector beams, cylindrical vector beams (CVBs) have beam of interest because their special polarization symmetry gives rise to unique high-numerical-aperture focusing properties that find important applications in nanoscale optical imaging and manipulation.[41] A general representation of a CVB including all descriptors is given by the equation,

$$\mathbf{E}_{\mathrm{C}} = \begin{pmatrix} \cos\left(p\ \alpha+\gamma\right) \\ \sin\left(p\ \alpha+\gamma\right) \end{pmatrix} e^{il\theta}, \tag{3.29}$$

where p is the order number or polarization rotational symmetry around the optical axis, which is an integer, l is the topological charge, and γ is a phase given by the state of polarization of the incident light beam. In this investigation, CVBs with topological charge $l = 0$ and polarization rotational symmetry $p = 1$ of types I and III are employed.[42] There are a number of passive and active methods to obtain these spatially structured vector beams. Among them, the use of S-waveplates is often found in the literature, Fig. 3.1. These devices work as a $\lambda/2$-retardation waveplate, but with a fast-axis oriented at an angle equal to the half of the local azimuthal angle. This polarization converter is also known as a vortex half-wave plate.[43] A Jones matrix representation is given as

$$\mathbf{S} = \begin{pmatrix} \cos\alpha & \sin\alpha \\ -\sin\alpha & \cos\alpha \end{pmatrix}, \tag{3.30}$$

where $\alpha = \arctan(y/x)$. It is straightforward that when an incident horizontal linearly polarized beam propagates through the S-waveplate, the transmitted beam is transformed to a radially linear polarized beam. This is,

$$\mathbf{E}_r = \mathbf{S}\,\mathbf{E}_H = \begin{pmatrix} \cos\alpha & \sin\alpha \\ -\sin\alpha & \cos\alpha \end{pmatrix} \begin{pmatrix} 1 \\ 0 \end{pmatrix} = \begin{pmatrix} \cos\alpha \\ \sin\alpha \end{pmatrix}. \tag{3.31}$$

Then, using Eq. (3.7) and $\chi = \sin\alpha/\cos\alpha = \tan\alpha$, it is found that

$$\tan 2\theta = \frac{2\Re\{\chi\}}{1 - |\chi|^2} = \tan 2\alpha. \tag{3.32}$$

Then, $\theta = \arctan(y/x)$. On the other hand, in order to obtain an azimuthal polarized vector beam, the polarization converter should be illuminated with vertical linearly polarized light. Thus,

$$\mathbf{E}_a = \mathbf{S}\,\mathbf{E}_V = \begin{pmatrix} \cos\alpha & \sin\alpha \\ -\sin\alpha & \cos\alpha \end{pmatrix} \begin{pmatrix} 0 \\ 1 \end{pmatrix} = \begin{pmatrix} \sin\alpha \\ -\cos\alpha \end{pmatrix}. \tag{3.33}$$

Consequently, $\chi = -\cot\alpha = \cot(\pi - \alpha)$ and

$$\tan 2\theta = \frac{2\Re\{\chi\}}{1 - |\chi|^2} = -\tan 2(\pi - \alpha). \tag{3.34}$$

Therefore, $\theta = \arctan(y/x) - \pi/2$.

3.4.1 Vector fields with CVBs

Vector holography requires the superposition of two electromagnetic waves with orthogonal states of polarization with propagation vectors subtending a small angle 2ψ.

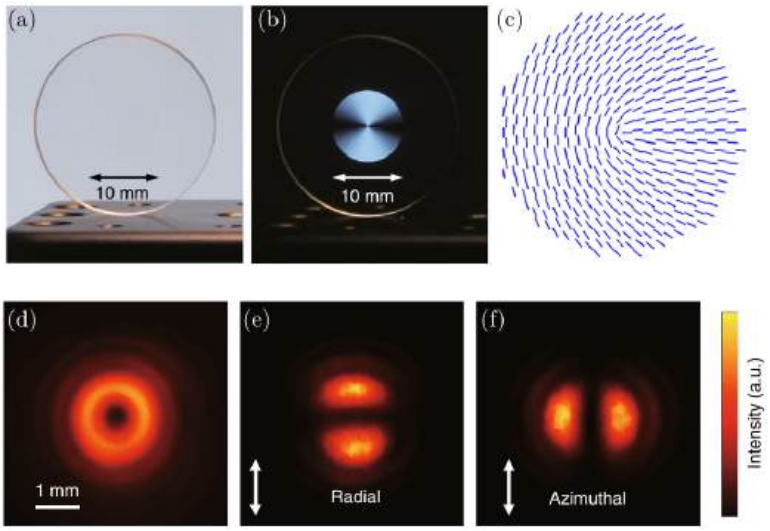

Figure 3.1: (a) S-waveplate without polarizing filters and (b) between cross linear polarizers. (c) Schematic showing the fast-axis distribution in the polarization converter introducing $\lambda/2$ retardation. (d) Unfiltered transmitted intensity by the S-waveplate when illuminated with linearly polarized light. (e) Transmitted intensity by a linear polarizer with its transmission axis vertical when polarization converter is illuminated with horizontal linearly polarized light and (f) with vertical linearly polarized light. Adapted from Refs. [44, 45]

Assuming one CVB with radial linear polarization and other with azimuthal linear polarization, its 3D-Jones vectors are given as

$$\mathbf{E}_{C_1} = \begin{pmatrix} \cos\alpha\cos\psi \\ \sin\alpha \\ \cos\alpha\sin\psi \end{pmatrix} e^{ik(x\sin\psi + z\cos\psi)}, \tag{3.35}$$

$$\mathbf{E}_{C_2} = \begin{pmatrix} -\sin\alpha\cos\psi \\ \cos\alpha \\ \sin\alpha\sin\psi \end{pmatrix} e^{ik(-x\sin\psi + z\cos\psi)}, \tag{3.36}$$

respectively. Then, the resulting vector field over the perpendicular plane to the angle bisector of the 2ψ angle at $z = 0$ is given as

$$\mathbf{E}_R = \begin{pmatrix} \left[\cos\alpha\, e^{ikx\sin\psi} - \sin\alpha\, e^{-ikx\sin\psi}\right]\cos\psi \\ \sin\alpha\, e^{ikx\sin\psi} + \cos\alpha\, e^{-ikx\sin\phi} \\ -\left[\cos\alpha\, e^{ikx\sin\psi} + \sin\alpha\, e^{-ikx\sin\psi}\right]\sin\psi \end{pmatrix} e^{-i\omega t}. \tag{3.37}$$

Tipically, z-component is neglected when recording angle and holographic recording medium thickness are small. Nonetheless, angle dependence in phase is significant to evaluate transverse spatial field modulation. Because photoinduced anisotropies, linear and circular birefringence, in recording films are proportional to intensity, conventional

Stokes parameters are locally derived through

$$S_0 = \langle E_{R,x} E_{R,x}^* \rangle + \langle E_{R,y} E_{R,y}^* \rangle \tag{3.38}$$

$$S_1 = \langle E_{R,x} E_{R,x}^* \rangle - \langle E_{R,y} E_{R,y}^* \rangle \tag{3.39}$$

$$S_2 = \langle E_{R,x} E_{R,y}^* \rangle + \langle E_{R,y} E_{R,x}^* \rangle \tag{3.40}$$

$$S_3 = -i \left[\langle E_{R,x} E_{R,y}^* \rangle - \langle E_{R,y} E_{R,x}^* \rangle \right] \tag{3.41}$$

where the time-dependent phase $e^{-i\omega t}$ was introduced previous to the time average, which is indicated by the angle bracket symbols $\langle \cdot \rangle$. $E_{R,x}$ and $E_{R,y}$ are x- and y-complex field components of resulting polarized field in Eq. (3.37) , the Stokes vector results

$$\mathbf{S} = \begin{pmatrix} \dfrac{12 + 4\cos(2\psi) + 8\cos(2kx\sin\psi)\sin(2\alpha)\sin^2(\psi)}{16} \\ \dfrac{4 - 4\cos(2\psi) - 4\cos(2kx\sin\psi)\sin(2\alpha)\left[3 + \cos(2\psi)\right]}{16} \\ \cos(2kx\sin\psi)\cos(2\alpha)\cos\psi \\ \sin(2kx\sin\psi)\cos\psi \end{pmatrix}. \tag{3.42}$$

It can be observed from S_3 that polarization ellipticity e is spatially modulated along x-axis and does not depend on the azimuthal angle α, but on the recording half-angle ψ. Besides, alternated changes in polarization handedness (blue ellipses for right-handed polarization and red ellipses for left-handed polarization) are well spatially modulated. This is more evident when $\psi \to 0$, because $S_3 \to \sin(2kx\sin\psi)$ and $S_0 \to 1$, finding that $e = \tan\left[0.5\sin^{-1}(S_3/S_0)\right] = \tan(kx\sin\phi)$. On the other hand, major semi-axis orientation ζ of the polarization ellipse is not clearly spatially modulated along the x-coordinate but depend on α. Applying again the above limit case, it is observed that $S_1 \to -\cos(2kx\sin\psi)\sin(2\alpha)$ and $S_2 \to \cos(2kx\sin\psi)\cos(2\alpha)$. Hence, $\zeta = 0.5\tan^{-1}(S_2/S_1) = 0.5\tan^{-1}\left[-\cot(2\alpha)\right] = \mathrm{sgn}\left[\cos(2kx\sin\psi)\right]\pi/4 + \alpha$, where $\mathrm{sgn}(x)$ is the sign function; then, ζ is piecewise constant along α but determined by x-coordinate. Figure 3.2 shows the spatial modulation described by Eq. (3.42), where blue ellipses represent right-handed polarization and red ellipses are for left-handed polarization.

3.4.2 Holographic recording

Spatially modulated vector fields require a photoanisotropic medium to be stored, namely, a material responsive to polarization of light. Azobenzene-containing polymer film, being a photoanisotropic medium, is initially isotropic, but changes its optical properties as a function of state of polarization of incident light. In general, linearly polarized light induces linear birefringence because of the perpendicular alignment of

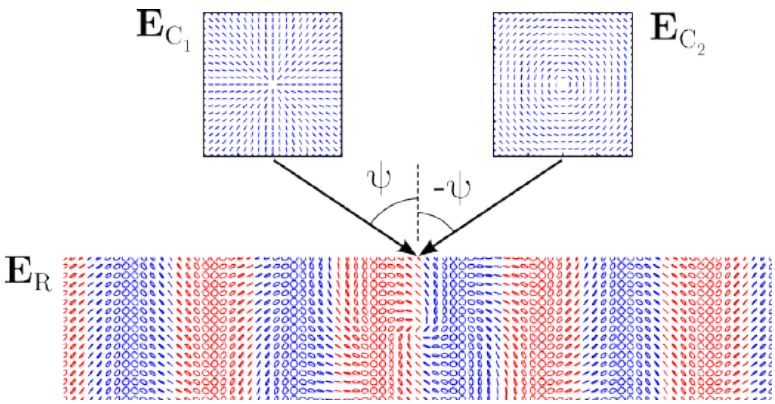

Figure 3.2: Vector field resulting from the superposition of radial and azimuthal linearly polarized fields.

azobenzene moieties with respect to the incident electric field vibration plane. Then, polymer photoanisotropic response can be modeled as

$$\Delta n_L = \eta I \sqrt{S_1^2 + S_2^2} = \eta I \cos\delta, \tag{3.43}$$

where η is the linear photoanisotropic constant, I is the total light intensity and $\delta = 2kx\sin\phi$ is the phase difference between the two orthogonally polarized recording vector beams. The fast-axis orientation angle is determined by the angle α subtended by the local major semiaxis of polarization ellipse and x-axis.

On the other hand, optical anisotropy induced by elliptically polarized light results in optical rotation mainly due to photoinduced chiral supramolecular structures, which are modeled as linear birefringent slabs with helicoidal fast-axis orientation in depth. Then, optical rotation provided by a polymer film of thickness d is given as

$$\theta = \tan(2\varepsilon)\frac{\Delta\phi_L}{2}, \tag{3.44}$$

where ε is the ellipticity angle of the recording polarized beam and $\Delta\phi_L = k\Delta n_L d$ is the linear retardance.[46] An additional term has been proposed to optical rotation given by Eq. (3.44),[47] but it seems that it is redundant because for fully polarized light it can be rewritten as

$$\theta = \frac{1}{2}kd\beta I S_3 = \frac{1}{2}\Delta\phi_C, \tag{3.45}$$

where $\Delta\phi_C = k\Delta n_C d$ is the circular retardance, $\Delta n_C = \beta I S_3 = \beta I \sin\delta$ is the circular birefringence, and β is the circular photoanisotropy constant. However, morphological features of the azobenzene-containing polymer condition the linearity of its chiral photoresponse.

A general approach to represent the photoanisotropic polarization hologram consists in calculating an infinitesinal generator $\mathbf{N}$ assuming that the governing Jones matrix $\mathbf{J}(z)$ of the recorded polarization hologram can be "exponentiated":[48]

$$\mathbf{J}(z) = \exp\left[i\mathbf{N}z\right], \tag{3.46}$$

where

$$\mathbf{N} = \left(\frac{\mathrm{d}\mathbf{J}}{\mathrm{d}z}\right)\mathbf{J}^{-1}. \tag{3.47}$$

When linear and circular diattenuation can be neglected, the total $\mathbf{N}$ Jones matrix can be obtained adding those obtained for linear and circular birefringence, namely, $\mathbf{N} = \mathbf{N}_L + \mathbf{N}_C$.[49] Applying Eq. (3.47) on Jones matrices for pure linear and circular birefringent media, it is found that

$$\mathbf{N}_L = ik\begin{pmatrix} n_1 & 0 \\ 0 & n_2 \end{pmatrix} = ik\overline{n}_L + ik\begin{pmatrix} \Delta n_L & 0 \\ 0 & -\Delta n_L \end{pmatrix}, \tag{3.48}$$

and

$$\mathbf{N}_C = ik\begin{pmatrix} 0 & -\Delta n_C \\ \Delta n_C & 0 \end{pmatrix}, \tag{3.49}$$

where $\overline{n} = (n_1 + n_2)/2$ is the average refractive index of the linear birefringent medium, $\Delta n_L = (n_1 - n_2)/2$ and $\Delta n_C = (n_l - n_r)/2$. With this at hand, the Jones matrix of the birefingent holographic grating using Eq. (3.46) results

$$\mathbf{J} = \begin{pmatrix} \cos B + i\Delta\phi_L\dfrac{\sin B}{B} & \Delta\phi_C\dfrac{\sin B}{B} \\ \Delta\phi_C\dfrac{\sin B}{B} & \cos B - i\Delta\phi_L\dfrac{\sin B}{B} \end{pmatrix}\exp\left(ik\overline{n}d\right), \tag{3.50}$$

where $B = \sqrt{\Delta n_L^2 + \Delta n_C^2}$.[50, 51] The above obtained Jones matrix is defined in the coordinate axes framework where photoinduced fast and slow axis coincide with x- and y-axis, respectively. Using the rotation matrix evaluated at the polarization ellipse orientation α, the Jones matrix representing the vector hologram can be transformed to be represented with respect the laboratory frame axes.[52] Therefore, assuming small photoanisotropic changes ($B \ll 1$),

$$\mathbf{J}_H = \begin{pmatrix} 1 - \Delta\phi_C\sin 2\alpha + i\Delta\phi_L\cos 2\alpha & \Delta\phi_C\cos 2\alpha + i\Delta\phi_L\sin 2\alpha \\ -\Delta\phi_C\cos 2\alpha + i\Delta\phi_L\sin 2\alpha & 1 + \Delta\phi_C\sin 2\alpha - i\Delta\phi_L\cos 2\alpha \end{pmatrix}. \tag{3.51}$$

Chapter 4

Experimental Methods

The experimental development was divided into 3 sections:

1. Polymer synthesis and film deposition:

   Azobenzene precursors were synthesized according to the methodology reported previously,[53] and briefly described elsewhere. From 4-hexyloxy or 4-hexil-substituted aniline and phenol by the azocoupling method, and in some cases it was made by the formation of an ether from a ω -bromoalcohol and an arylalcoholate to add a spacer group. Azomonomers were prepared through the formation of an acrylate from an allyl halide and an azobenzene precursor. Azopolymers were obtained by free radical polymerization of an azomonomer at 65 ° C for 48 h using AIBN (3% for each reaction) as initiator and DMF as solvent. To purify azopolymers, they were precipitated twice in methanol, filtered and dried in a vacuum oven. Materials were characterized through Nuclear Magnetic Resonance (NMR), Fourier-transform infrared spectroscopy (FTIR), Thermogravimetric analysis (TGA), Differential scanning calorimetry (DSC), and average molecular weights (Mn and Mw) of azopolymers were measured by size exclusion chromatography (SEC). The photoreactive films were prepared by drop-casting a THF solution with and adequate concentration of azopolymer powder product.

2. Optical characterization:

   Rotating-waveplate-based Stokes vector and Mueller matrix imaging polarimetry were implemented to characterize diffracted vector fields and photoinduced anisotropy in azopolymer films, respectively. Through Mueller matrix decomposition at each pixel, an spatial mapping of elementary optical anisotropies (such as diattenuation and birefringence) were determined. Also, atomic force microscopy

was used to explore film surface in order to determine the formation of a relief modulation.

3. Polarization holographic recording:

   An experimental interference setup was implemented to superimposed, at least, two laser beams with proper wavelength and having propagation vectors subtending a small angle onto an azopolymer film. With the aim of producing spatially modulated vector fields over the superposition region, polarization elements (linear polarizers, Berek compensators, S-waveplates) were used through beam trajectories to produce orthogonal states of polarization in interference beams. Measurement of diffraction efficiency of holographically recorded polarization elements were implemented by using a laser probe beam with wavelength far from the absorption band, previously determined by UV-Vis spectroscopy, of azopolymer films.

4.1 Polymer synthesis and film deposition

Azobenzenes are molecules with very interesting characteristics that have attracted attention due to the wide variety of colors that can be obtained by varying the substituent groups attached to the aromatic rings. Initially, they were primarily used as dyes. These compounds are classified within the azo-aromatic compounds, which also include compounds such as aminoazobenzene and pseudo-stilbenes.[54] The UV absorption spectrum of an azobenzene exhibits two characteristic absorption bands, corresponding to the electronic transitions $\pi \rightarrow \pi^*$ and $n \rightarrow \pi^*$.[28] The $\pi \rightarrow \pi^*$ transition is generally found in the near-UV region and is also common to referable carbon systems such as stilbene.[55] The electronic transition called $n \rightarrow \pi^*$ is usually located in the visible region, and is due to the presence of the unshared electron pair of the nitrogen atoms. This second electronic transition causes azobenzenes to have a dynamic photoisomerization process different from carbon systems.[56] In Figure 4.1, the molecular structure shows the two configurations of geometric isomers, the trans form (E), and the cis form (Z), the first one is the most stable thermodynamic isomer.

For this section, a colaboration with Centro de Investigación en Química Aplicada (CIQA) was carried out, in Saltillo, Coahuila. Through the polymer synthesis, 5 polymers containing azobenzene units in their side chain were obtained: POC6-0 (LMW), POC6-0 (HMW), PC6-0, POC6-6, POC6-2.

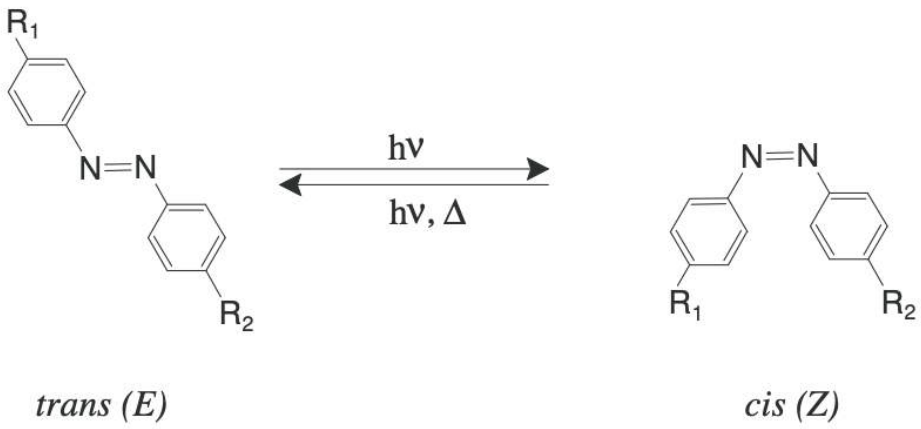

Figure 4.1: *Trans* and *cis* geometric isomers of an azobenzene derivative.[32]

All reactions were carried out using the same methodology (see Fig. 4.2,for which the same variables were set for all cases. The polymerization reactions of the different synthesized monomers were carried out by the classical free radical polymerization method using the *Schlenk* technique, using Anhydrous Dimethylformamide (DMF) as the reaction medium in sufficient quantity to dissolve the reagents, and AIBN as the initiator in a ratio of 2-3% mol with respect to the monomer. The reagents were weighed (500 mg of monomer) and placed in a *Schlenk* flask with a magnetic stirrer; it was placed for 5 minutes in an ultrasonic bath to start the reaction. The system was put under vacuum to remove air and then, with the help of an argon balloon, it was placed in an oxygen-free atmosphere. The system was degassed 3 times by freeze-pump-thaw cycles, to remove oxygen. Before that, system was saturated with argon gas to maintain an inert atmosphere, and then the reaction mixture was heated to 65°C during 40-44 hours.

The polymer was purified by precipitation in 80 ml of mixed of destilled water and methanol (1:1), re-dissolved in chloroform and re-precipitated in 100 ml of methanol. Third precipitation was carried out in 100 ml of hexanes. Finally it was dried and characterized. The yields obtained were on average ±50%.

For the measurement of optical properties, two types of films were prepared. For this purpose, solutions with a concentration of 40 mg/mL were prepared, using solvents such as THF (Tetrahydrofuran) and spectroscopic grade chloroform. The first type of films prepared was by the evaporation method (casting) (Fig. 4.3), which consisted of depositing 100 μl on a previously washed and leveled glass substrate, so that the solution homogeneously covers the entire surface of the substrate, allowing them to dry afterwards, thus obtaining thick films. The second type of films prepared was by means

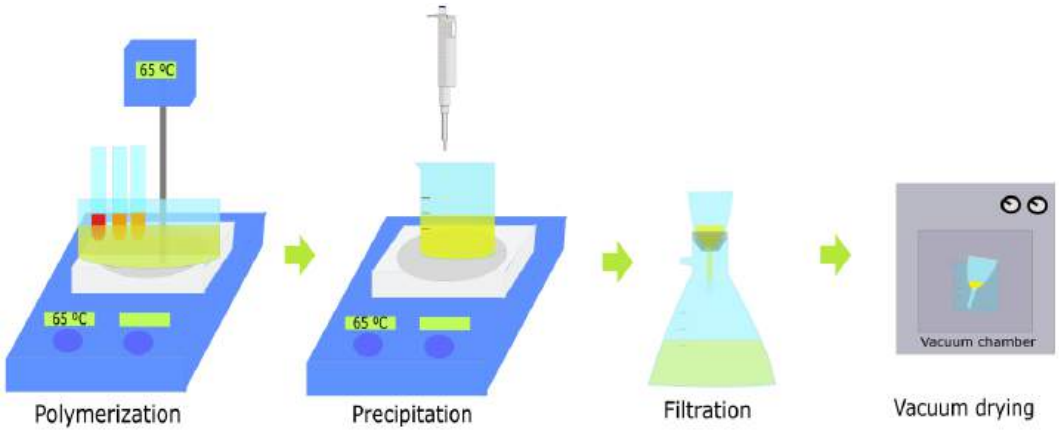

Figure 4.2: Polimeryzation Process

of the spin-coating technique, using a centrifuge on which a quartz substrate was fixed and 120 μl of sample was deposited in the center of the substrate.

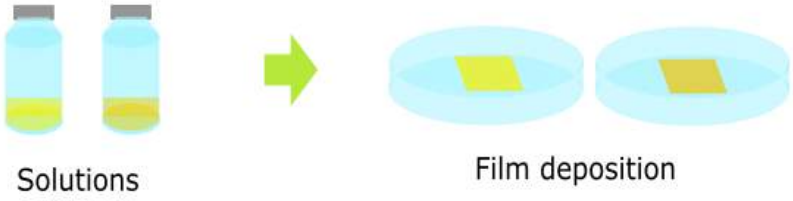

Figure 4.3: Film Deposition

4.2 Optical Characterization

In this section, methods and optical setups used to characterize optical properties of holographic recording media are described. First, the experimental arrangement for measuring the photoinduced birefringence was employed to obtain the photoalignment rate of the synthetized azopolymers during illumination with a linearly polarized laser beam in order to prove that these materials have photoanisotropic properties. After this birefringence measurement, an imprint of the radial/azimuthal linearly polarized beam generated with the S-plate was obtained in the azopolymer film to verify that the material was recording information correctly. Finally, after establishing the optimal exposure, the photoinduced radial/azimuthal anisotropies were read using an optical arrangement designed so that the transmitted beam could be analyzed using Stokes polarimetry.

4.2.1 Photoinduced anisotropy

An optical arrangement was set up to follow the photoinduced birefringence kinetics in the azobenzene polymer films (Fig.4.4). Two continuous-wave laser light sources were placed orthogonally, each providing electromagnetic radiation at convenient wavelength to have simultaneous lecture with one of them and writing with the other one. The former beam with a center wavelength λ_r of 633 nm (red color) far from absorption bands, and the latter with a center wavelength λ_w of 488 nm (blue color) at the absorption bands. Next, two linear polarizers (LP) were placed at the output of each light source with the aim of ensuring linear polarization at both propagating beams. A dichroic mirror (DM) was positioned tilted at the crossing point between the laser beam paths, which has the function of reflecting a certain wavelength and transmitting a different one; in this case, the red beam passes through and the blue beam reflects, working as an optical long-pass filter. At this point, it is necessary to warrant that the excite and probe beams propagate collinearly throughout the entire path. Then, the azopolymer film (S) was placed at the beam paths, followed by another dichroic mirror (DM) identical to the first one but perpendicularly to propagation paths. In consequence, the output signal was only the red beam that was collected with a monolithic Stokes polarimeter, connected to the computer where the birefringence curve was obtained and analyzed with the help of Matlab suite.

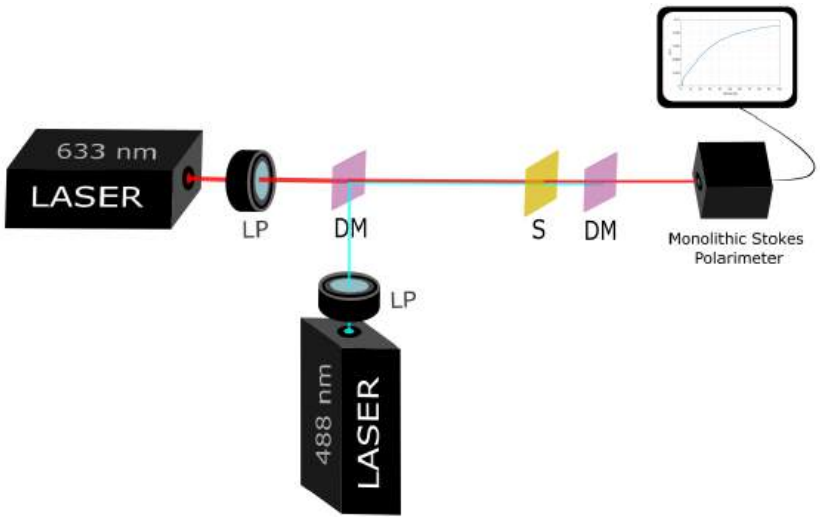

Figure 4.4: Experimental set up for measurement of photoinduced birefringence

4.2.2 Cylindrical vector beam imprint

Then, an optical arrangement was made for the engraving of the cylindrical vector beam generated with a S-waveplate on the azopolymer film, (Fig. 4.5). This radial polarization converter is a phase plate that converts a homogeneous linearly polarized beam in a beam with radial or azimuthal distribution of linear polarization states in its cross section. This is possible because the optical device shows radial birefringence, where the fast axis is oriented radially. The writing beam (488 nm) was aligned, followed by a linear polarizer (LP) oriented horizontally; then, a beam expansor (E), this to make the beam diameter larger and the record had a larger area, thus being more visible. Later, a half-wave retarder (HW) was placed, which changes the orientation of the beam polarization; however, on this occasion it was oriented in the same way, at 0°; an S-plate (SP) and finally the sample, which in this case is the azopolymer film (S). The film was left recording for approximately 4 hours.

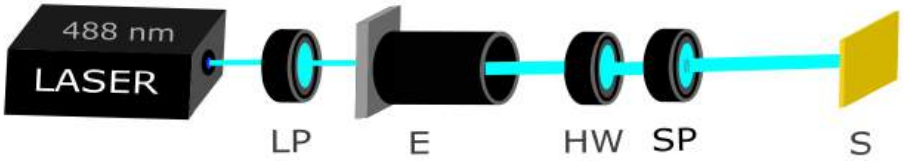

Figure 4.5: Optical arrangement for replica registration of an S-Plate

After this time, an optical arrangement was made for the analysis of the previously recorded imprint, where instead of the writing laser, the reading beam (633 nm) was placed and propagated through a linear polarizer (LP), a beam expander (E) and a half-wave retarder plate (HW). Then, the sample (S) was placed (Fig.4.6) taking care that the beam was completely aligned, covering the same area where the writing beam had been recording. In this configuration, a Stokes polarimeter was placed after the sample, device that comprises a rotating quarter-wave plate, a linear polarizer and a photosensitive sensor array. The retarder fast-axis orientation was synchronized with the image capture with a CMOS camera and stored in a computer with the aim of building a image cube for future pixel-by-pixel Fourier analysis.

4.3 Polarization and Holographic recording

For the hologram recording, a new arrangement was configured, which is shown in Fig. 4.7. A well-aligned Ar-ion laser beam with a wavelength of 488 nm (blue) was propagated through a 10X beam expander (E) and a Berek compensator (BC), the

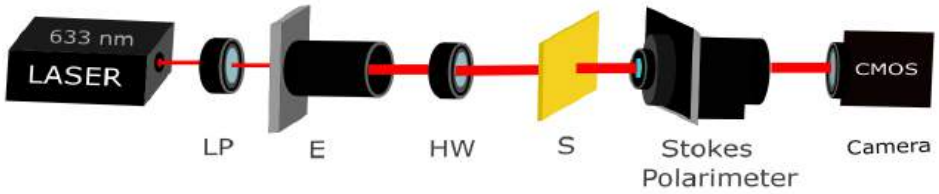

Figure 4.6: Optical arrangement for reading registration of an S-plate

latter being used to generate a horizontally oriented linearly polarized beam. Then, light passed through a half-wave retarder plate (HW) to control linear polarization orientation. Next, a S-waveplate (SP) introduced a radial modulation of the orientation angle of linear polarization. This cylindrical vector beam was then separated in two identical replicas by a nonpolarizing 50:50 beam splitter cube (BS), in which half of the beam power was transmitted and the other part was reflected. The reflected light beam was directed to a mirror (M) tilted conveniently so that the once-again reflected beam and the transmitted beam by the BS were superimposed subtending their propagation vectors an angle less than 5°. Finally, the latter vector beam was transformed by a liquid crystal optical rotator (LCR), whose function is to rotate 90° the linear polarization orientation angle. In this way, two orthogonal cylindrical vector beams were obtained. The side-chain azobenzene-containing polymer film was then placed exactly where both beams overlapped. The sample was exposed to the resulting vector vortex field for approximately 7 hours.

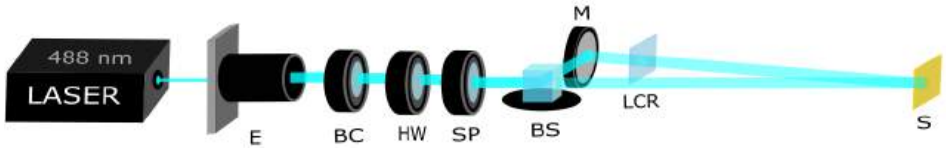

Figure 4.7: Optical arrangement for Hologram recording

In order to visualize photoinduced optical anisotropies, Mueller imaging polarimetry was implemented. The polarimetric device used the measurement principle of two rotating quarter-wave retardation plates to characterize the holographic vortex vector grating photoinduced in the azopolymer films. The illumination source was a 3 W red LED emitting at a center wavelength of $\lambda = 635$ nm and bandwidth $\Delta\lambda = 30$ nm. Then a collimating system, comprising a condenser and an achromatic convergent doublet, was optimized. The plane wave was propagated through a polarization state generator made of a linear polarizer and an achromatic rotating quarter-wave retarder. The generated polarized beam illuminates the recorded azopolymer film and

the transmitted beam carried the modulated anisotropy information. Here, a number of intensity photograms were captured to build an image cube. This image stack was Fourier analyzed pixel by pixel considering the angle shift ratio between the quarter-wave retarder in the polarization state generator and analyzer. Then a microscope objective with a magnification of 40x was placed, followed by a Stokes polarimeter. The latter was build with a rotating $\lambda/4$-retarder plate and a linear polarizer. Finally, the CMOS camera was placed. Once the Mueller matrix images were retrieved and after a polar decomposition of the Mueller matrix at each pixel, spatial mappings of the uncoupled elementary optical anisotropies (such as diattenuation and birefringence) were obtained.

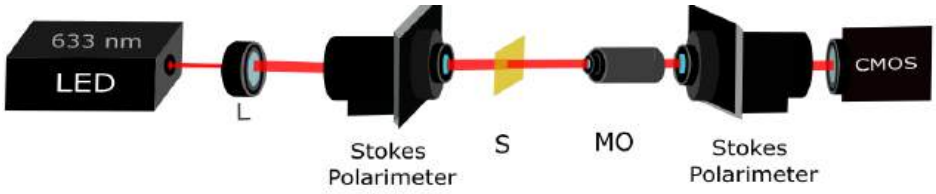

Figure 4.8: Optical arrangement for Hologram lecture with Mueller Polarimetry

To evaluate the polarization characteristics of the diffracted field at the hologram reconstruction stage, imaging Stokes polarimetry was used. In this setup, a 1 cm-diameter 642 nm laser beam was used as a light source and aligned. It was propagated through a linear polarizer (LP) with its transmission axis oriented at 0°, and a half-wave retarder plate to control the azimuth of linearly polarized light. A q-plate designed to work properly at red wavelength was employed to generate a probe cylindrical vector beam. The azobenzene-containing polymer film was then placed and illuminated by the previously generated beam just in the area where the vector hologram was recorded. A number of transmitted diffraction beams were observed. Next, the imaging Stokes polarimeter previously described was placed to analyze only the first-diffraction order and the spatial modulation of the state of polarization over its cross section determined, see Fig. 4.9.

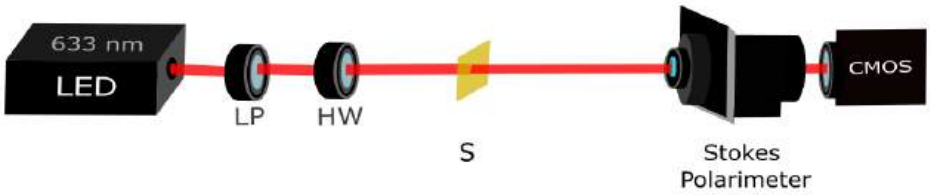

Figure 4.9: Optical arrangement for Hologram lecture with Stokes Polarimetry

Chapter 5

Results

5.1 Introduction

In this section the results obtained from this research will be shown, where an analysis of the characterization of the synthesized polymers will be given. Chemical structure and purity were confirmed by Proton Nuclear Magnetic Resonance (^{1}H-NMR), and results attested that residual monomer was eliminated. Molecular Weight of synthesized polymers were determined by Size Exclusion Chromatography (SEC), obtaining values between 8,000 and 14,000 g/mol (Mn), (see Table 3.2). Those molecular weights are typical for polymers synthesized via free-radical polymerization. It is important due to an increment of molecular weight increase viscosity of polymer and decrease mobility of molecules that diminish optical properties.

Table 5.1: SEC and TGA characterization of different synthesized polymers.

Polymer	Mn (g/mol)	Mw (g/mol)	IP [Mw/Mn]
POC6-0 (LMW)	8036	10607	1.32
POC6-0 (HMW)	13155	23290	1.77
POC6-2	10427	15736	1.51
POC6-6	10908	16093	1.47
PC6-0	14208	28837	2.03

After that, the measurement and analysis of the photoinduced birefringence that this material has will be shown, where the birefringence curve obtained by means of the optical arrangement described in the previous chapter can be observed (4.4) Later the vector beam recorded in the thin film of Azopolymer will be shown. Finally, details of the recorded vector vortex hologram and its analysis using Mueller polarimetry will be revealed, where some anisotropic properties of this material will be shown, such

as diattenuation, birefringence and depolarization (4.8). In order to later make a reconstruction with the help of Stokes polarimetry. (4.9)

5.2 Polymer thermogravimetric characterization

As it was mentioned, five polymers containing azobenzene moiety in their side chain were synthesized. These were labeled as POC6-0 (HMW), POC6-0 (LMW), PC6-0, POC6-6, POC6-2 considering substituent and spacer length in the notation. In a simplistic way it can be said that substituent is related to molecule conjugation while spacer length with side-chain mobility. An scheme of their molecular structure is shown in Fig. 5.1. The former two polymers have either the same molecular structure, the difference between them is the molecular weight.

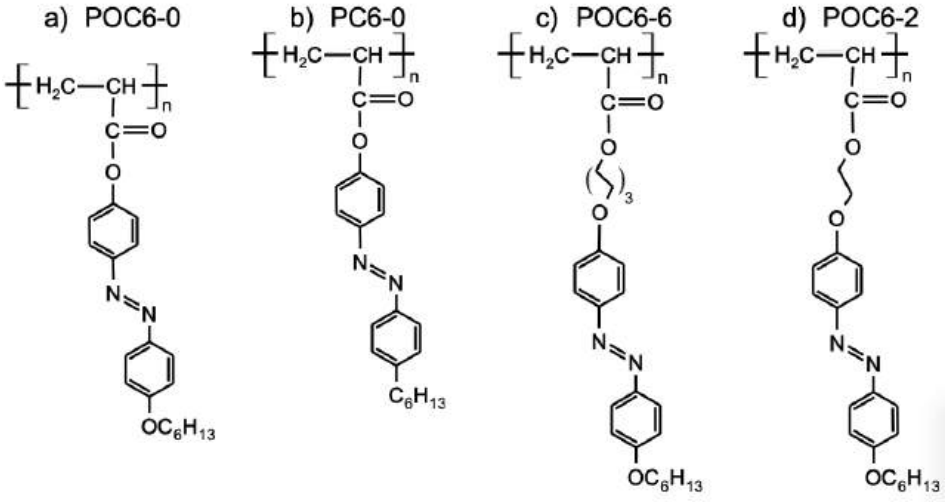

Figure 5.1: a) POC6-0 polymer chain, b) PC6-0 polymer chain, c) POC6-6 polymer chain, d) POC6-2 polymer chain

One characteristic of the process to obtain these kind of polymers is that the product have high molecular weight and a greater resistance to degradation. For that reason, the azopolymer series was characterized through thermogravimetric analysis (TGA), which is one of the thermal analysis techniques used to characterize material such as polymers. It measures the velocity of change in the mass of a sample as a function of temperature or time in a controlled atmosphere. The characterization results through this technique are shown in Fig. 5.2

In Fig. 5.2 a), it is observed that polymer POC6-0 shows thermal stability below a temperature of 277°C before it starts to degrade. The TGA curve for the polymer PC6-0, Fig. 5.2 b), indicates that it can endure without suffering any thermal damage

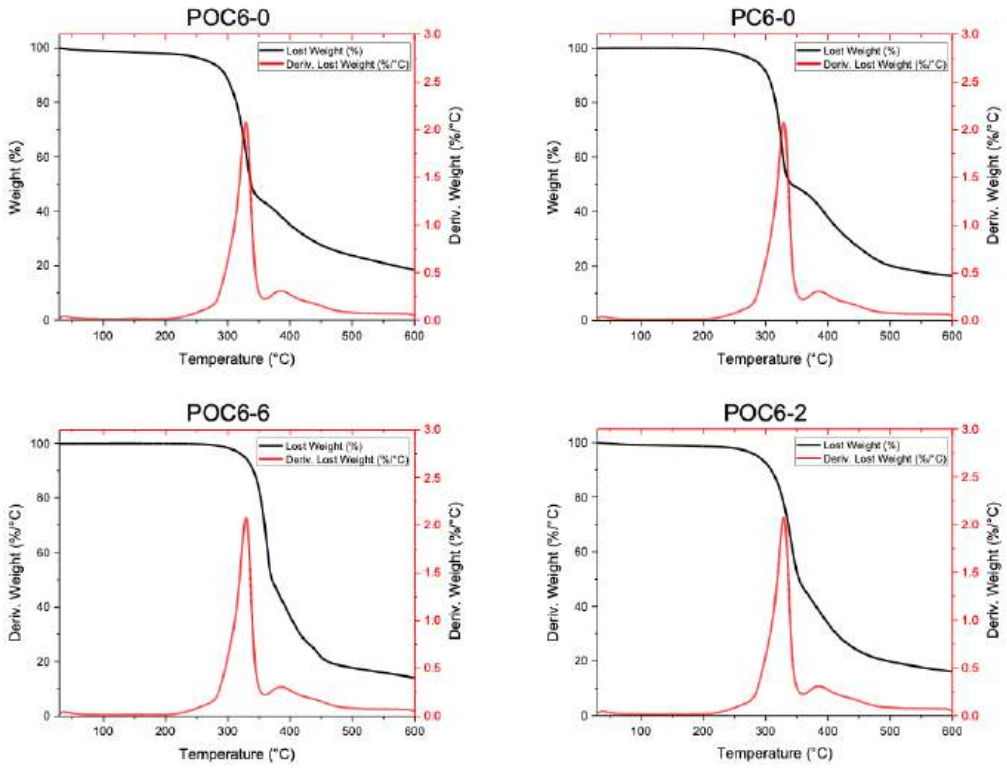

Figure 5.2: Thermogravimetric Analysis (TGA) of 4 Azopolymers.

until 254°C. On other hand, TGA for polymer POC6-6 in Fig. 5.2 c) reveals that the temperature threshold to observed decomposition is 310°C. Finally, POC6-2 polymer shows that before suffering any damage, it can endure 260°C. With this results we can conclude that the degradation temperature that these polymers have is very high allowing the manipulation at room temperature, around 25°C, without suffering any damage. Besides, to our knowledge, the accumulated heat by the absorbed fluence does not reach to generate these temperatures. For example, it has been reported more than 10,000 write/erase cycles, some in azopolymers.[57]

5.3 UV-Vis absorbance spectroscopy

In order to identify the $\pi - \pi^*$ and $n - \pi$ bands that are related to trans- and cis-isomer populations, respectively, the absorbance of the polymer series was obtained. In these five different absorption curves (Fig.5.3), it can be observed that POC6-0 (HMW) and POC6-0 (LMW) polymers are the two that have a better response at beam irradiation with a wavelength of 488 nm. It can be seen that the writing beam coincides with the final part of the curve of the $n - \pi$ band, which is directly related to the *cis* isomer. On the other hand, wavelength of the reading beam is far from absorption peaks with

the aim of avoiding the interference with the recording process. It should be pointed out that better absorption and, consequently, high photoalignmen rate through trans-cis-trans isomerization process can be reached with shorter wavelengths. However, the optical element to be used in the holographic application is designed to work at a center wavelength of 488 nm.

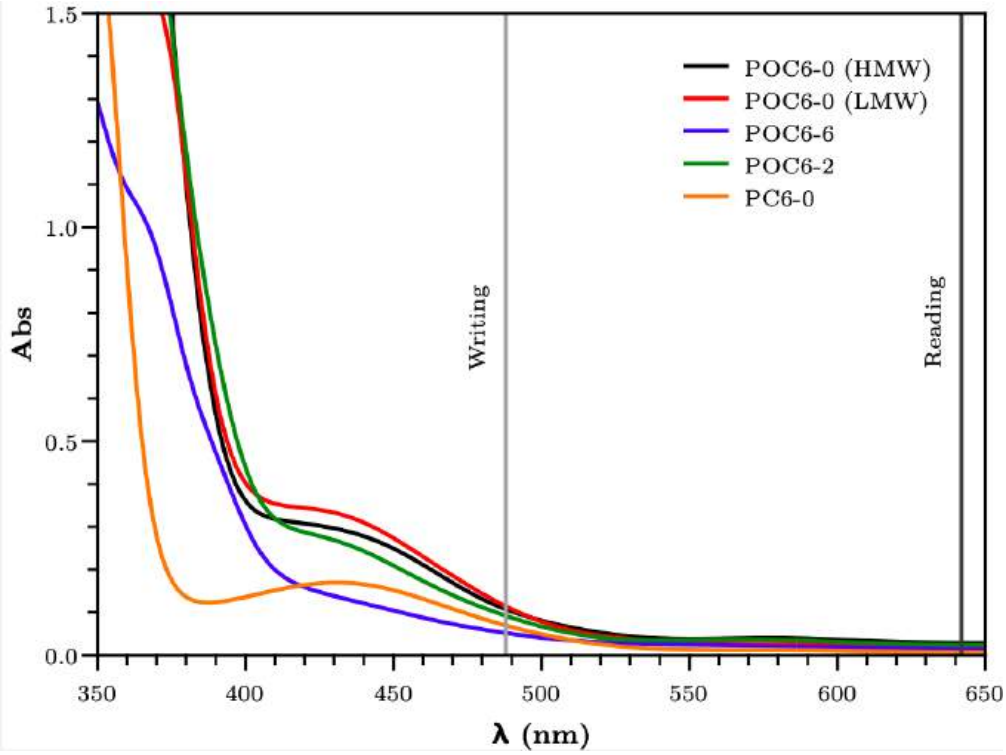

Figure 5.3: Absorbance spectrum of polymers obtained in thin films

An additional feature of these spectra consists in that it is possible to identify the effect of the substituent in the polymer film absorption. For example, cis- and trans-isomer bands are clearly separated in polymer PC6-0 that it is not the case for the rest of the series. Thus, the oxygen-substituent produces broader absorption bands that perceptibly overlap. Otherwise, the longer space length reduce notably the cis-to-trans isomer population ratio in polymer POC6-6. It may be because the available free volume allows the azobenzene molecule to be preferentially in the trans-isomer conformation, because the cis-isomer is less stable.

5.4 Photoinduced linear birefringence

Anisotropic photoresponse was evaluated by using the polarimetric setup described in Section 3.7 where the writing (excitation) beam was provided by a tunable Ar-ion

laser set at 488 nm and the reading (probe) beam was delivered by a semiconductor laser at 635 nm. Both beams were manage to have linear polarization after being transmitted/reflected by the tilted dichroic mirror employing Berek compensators. The writing beam was set to be vertically (perpendicular to the optical table) polarized and the reading one to have an orientation of 45° with respect to the optical table. The writing beam was blocked by the second dichroic mirror, placed in front of the Stokes polarimeter, and the reading one was measured. The Stokes polarimeter logs, among other data, the four parameters each 30 ms (approximately). It is expected that azobenzene moieties in the photoreactive film align perpendicularly to the writing polarized beam, increasing the effective refractive index in the horizontal direction (x-axis parallel to the optical table), namely, a photoinduced birefringence is obtained. Then, the x-component of the reading beam will be retarded with respect to the y-component and the transmitted beam is transformed to an elliptically polarized beam with right-handedness.

Photoinduced birefringence can be determined, assuming no diattenuation, through the following Mueller matrix analysis. The mathematical representation of the problem is given as

$$\begin{pmatrix} I_o \\ Q_o \\ U_o \\ V_o \end{pmatrix} = \begin{pmatrix} 1 & 0 & 0 & 0 \\ 0 & 1 & 0 & 0 \\ 0 & 0 & \cos(\Delta\varphi) & \sin(\Delta\varphi) \\ 0 & 0 & -\sin(\Delta\varphi) & \cos(\Delta\varphi) \end{pmatrix} \begin{pmatrix} 1 \\ 0 \\ 1 \\ 0 \end{pmatrix}. \tag{5.1}$$

where $\Delta\varphi = k\Delta n d$ is the retardance, being $k = 2\pi/\lambda$ the wavenumber, Δn the linear birefringence of the anisotropic medium, and d the film thickness. From the above, it is straightforward that the photoinduced retardance can be known from

$$\Delta\varphi(t) = -\tan^{-1}\left(\frac{V_o(t)}{U_0(t)}\right). \tag{5.2}$$

Time dependence has been included in order to make explicit the photoalignment rate. It is important to clarify that these measurements were carried out on films made using the spin coating method, resulting in thinner films, shorter recording time even when using low writing power, and weak photoinduced retardance.

In Fig. 5.4, the photoresponse under identical conditions for the polymer series is presented. Polarimetric data have been normalized because saturation level and kinetics slope are key features to compare photoresponsivity. However, photoinduced birefringence rate is proportional to the shown plots. It can be observed that the better performance is shown by azopolymer POC6-0 (LMW), while the worst is obtained for the POC6-6 azopolymer that also shows the lower absorbance at 488 nm. On

the other hand, POC6-0 (HMW) shows a lower photoresponse than POC6-0 (LMW) may be because the higher polymer molecular weight prevents a faster and higher photoalignment rate.[58] .Substituent is also a factor that affects photoresponse, as it is demonstrated by induced photoalignment rate of PC6-0. Further research, beyond the scope of this thesis, needs to be done with the aim of optimizing polymer molecular conformation. At this stage, azopolymer POC6-0 (LMW) was chosen to record the holographic vector vortex grating.

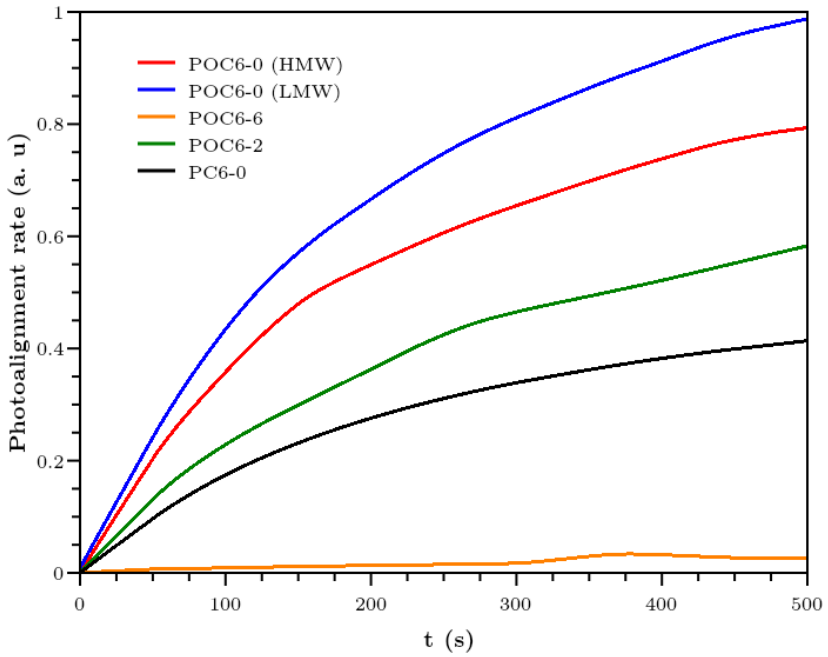

Figure 5.4: Photoalignment rate for the series synthesized of side-chain azobenzene-containing polymer films obtained through spin coating.

5.5 Cylindrical vector beam imprinting in azopolymer thin film

A previous step to record the holographic vector vortex grating was to evaluate the optical imprinting of cylindrical vector beams into the side-chain azobenzene-containing polymer film. The recording media were obtained by the casting method resulting a thicker film.

An optical arrangement was made for the engraving of a replica of the S plate on the Azopolymer film (Fig. 5.5)). This S plate is a plate that induces polarization states, where the fast axis is oriented radially. The writing beam (488 nm) was aligned, followed by a linear polarizer (LP) oriented horizontally (0^{o}), followed by a beam expansor (E),

this to make the beam diameter larger and the record had a larger area, thus being more visible. Later, a half-wave retarder (HW) was placed, which changes the orientation of the beam polarization, however on this occasion it was oriented in the same way, at 0^{o}; an S plate (SP) and finally the sample, which in this case is the POC6-0 Azopolymer film. (S).The film was left recording for 2 hours.

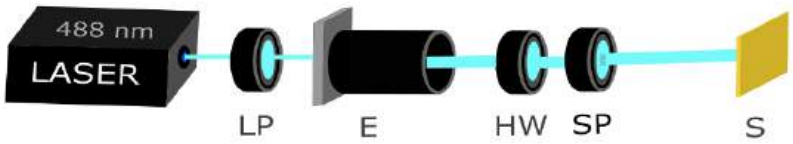

Figure 5.5: Vector Beam recording arrangement

After this time, an optical arrangement was made for the analysis of the previously recorded replica (Fig. 5.6, where instead of placing the writing laser, the reading beam (633 nm) was placed. Followed by the linear polarizer (LP), the beam expander (E) and the half-wave retarder plate (HW), then the sample (S) was placed, taking care that the beam was completely aligned, covering the same area where the writing beam had been recording. In this configuration, after the sample, a Stokes polarimeter was placed, consisting of a quarter-wave plate and a linear polarizer, and this in turn was connected to a CMos camera, which was in charge of capturing the necessary images for future analysis by Stokes polarimetry.

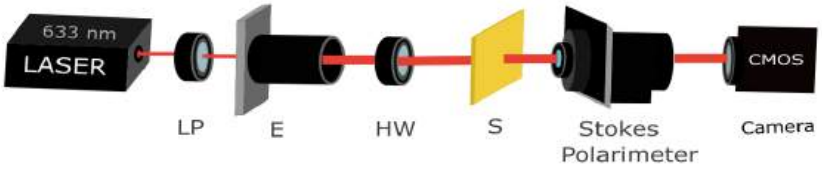

Figure 5.6: Vector Beam lecture arrangement

When the film is irradiated with the reading beam (633nm), circular polarization states are obtained as can be observed in Fig. 5.7, in the 4th Stokes parameter (S3) where the S plate is completely replicated in the Azopolymer film, it is observed that it has the ability to record circular polarization,

5.6 Holographic vector vortex gratings: Recording and evaluation

Previous efforts to record a holographic polarization grating by superposition of two orthogonally polarized vector vortex beams in photo-crosslinkable polymer liquid crystal

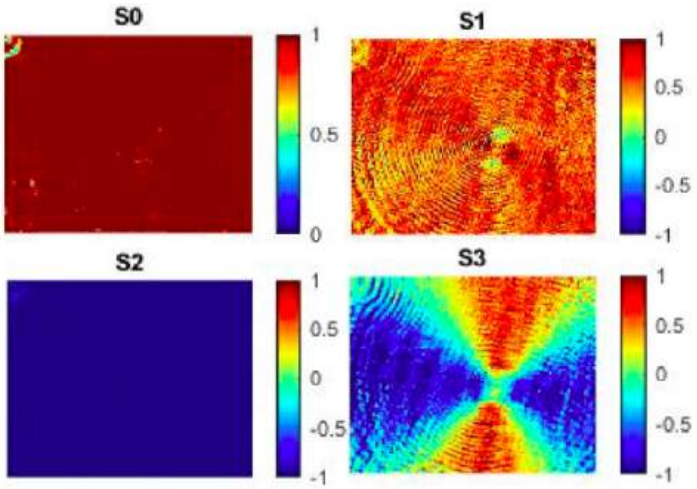

Figure 5.7: Stokes parameters analysis of POC6-0 Polymer film

with 4-(4-methoxycinnamoyloxy)biphenyl side groups as a polarization-sensitive material have been reported in the literature.[52] Nonetheless, the photosensitive material is inefficient to follow circularly polarized light.[59] These features limit the holographic recording process when two orthogonal linearly polarized beams are superimposed. Besides, it is known that to generate a vortex light beam it is necessary an amplitude or phase fork grating which induces a helical phase into an incident Gaussian plane wavefront.[60, 61] In order to obtain a vortex vector beams it is necessary to superimpose left and right circularly polarized vortex beams.

Herein, the holographic vector vortex grating was inscribed in a side-chain azobenzene-containing polymer film, which was polarimetrically evaluated using the Mueller matrix imaging microscopy. Imaging system have been aligned with the center of the holographic recording, location where the discontinuity is expected. A total of 16 images, see Fig. 5.8, representing the spatial distribution of each Mueller matrix coefficient were obtained. At first glance, it is observed a double fork modulation, one of them pointing upwards and the other downwards. Consequently, it is expected that this vector hologram produce an structured beam by diffracting an incident reading beam. In addition, there is a modulation shift corresponding to a quarter of the grating spatial period in some Mueller coefficients. This is a characteristic of linear and circular anisotropic properties induced by the spatial distribution of linearly and circularly polarized light, respectively, predicted by the model. To our knowledge, this anisotropic response reveals a characteristic that had not been achieved before in other photoresponsive materials when recording a polarization holographic grating. For this holographic recording, the azopolymer film deposited by casting was POC6-0 (LMW),

which gave a better response in the various tests previously conducted.

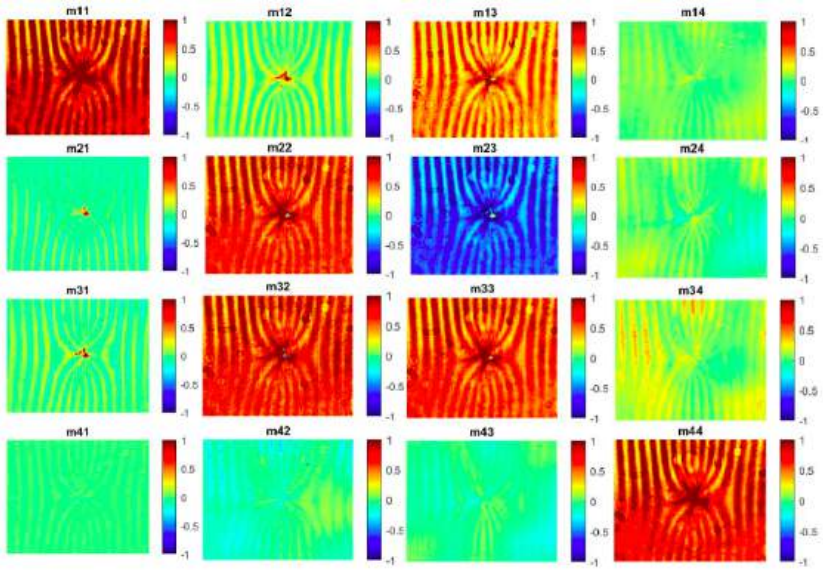

Figure 5.8: Mueller Matrix

Because all of the Mueller matrix coefficients show some degree of spatial modulation, it is expected that three different anisotropy properties were photoinduced into the azopolymer film: diattenuation (D), depolarization (Δ), and birefringence (R). Then, an approach to decoupled this optical properties consider that the Mueller matrix $\mathbf{M}$ at each pixel is separable. Thus,

$$\mathbf{M} = \mathbf{M}_{\Delta}\, \mathbf{M}_{R}\, \mathbf{M}_{D}, \tag{5.3}$$

and through some matrix properties and transformation, known as the polar decomposition method [62], each basic anisotropy can be retrieved.

In Fig.5.9, the resulting images obtained from these three optical anisotropies calculated pixel by pixel from the corresponding Mueller matrix are shown. First, total diattenuation is presented, followed by linear diattenuation, and then circular diattenuation. In this parameter, modulation (distribution of polarization states, as shown in the theoretical model) can be observed, confirming that the experimental model was correctly applied. Besides, in the latter image, there is some regions where the grating spatial frequency is doubled as consequence of overexposure.

In the second row, related to depolarizance, it is observed significative linear depolarization values. On the other hand, total retardance seems to have an uniform spatial distribution. However, when linear and circular birefringence are separated, it is observed an spatial modulation of the linear and circular anisotropic properties, which are complementary distributions.

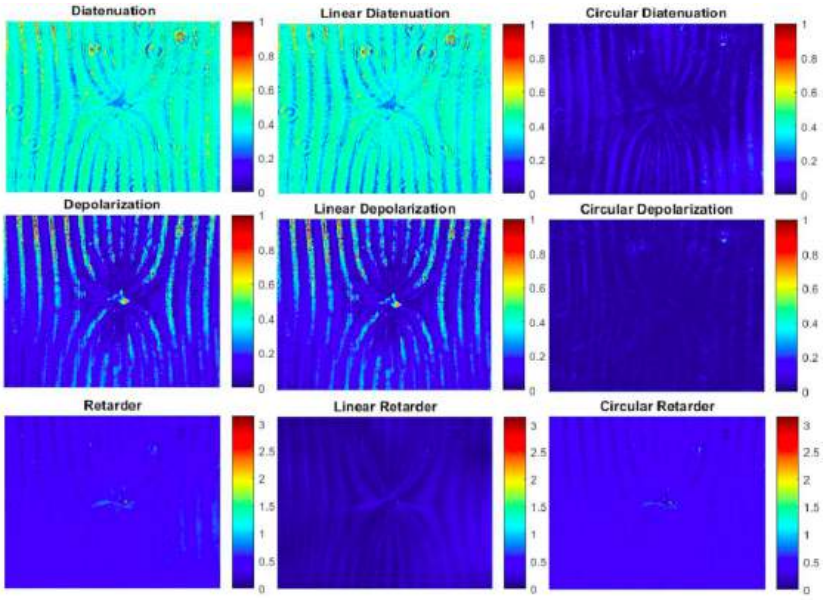

Figure 5.9: Anisotrophy Measures

Hologram reconstruction was first numerically implemented using the results derived in Subsection 3.4.2, by Fourier transforming x- and y-components of incident vortex electric field. The simulated Stokes parameters in the diffracted beam are shown in Fig.5.10

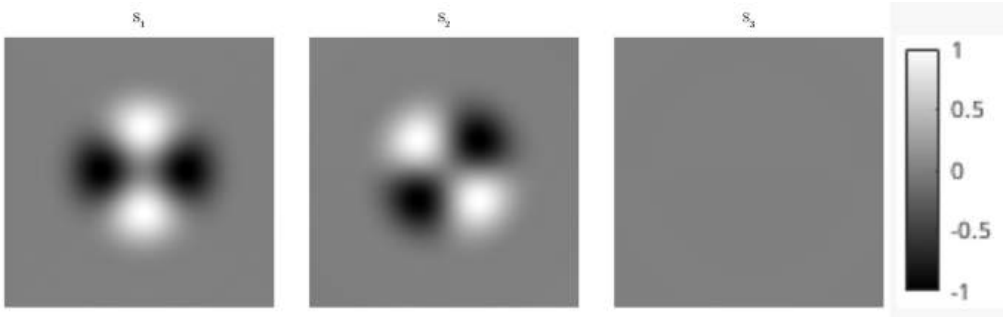

Figure 5.10: Simulated Stokes Parameters in the diffrated beam

Trough Stokes polarimetry, it was possible to reconstruct the hologram previously recorded on an azobenzene film, which was POC6-0. In Fig.5.11, the four Stokes parameters can be seen. For this analysis, one of the two beams is obstructed, illuminating with only one and obtaining the reconstruction of the one that is being blocked.

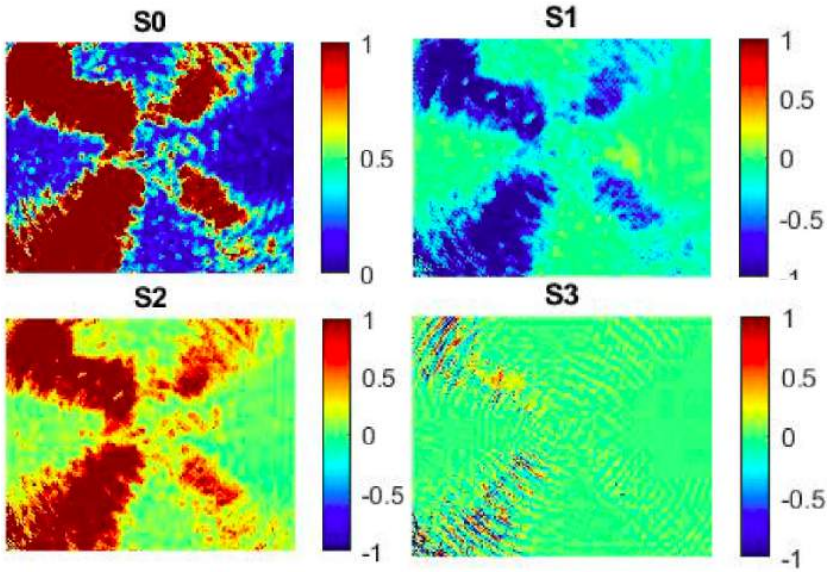

Figure 5.11: Vector beams reconstruction through Stokes Polarimetry

Chapter 6

Conclusion

6.1 Summary of the Study

In this research, a side-chain azobenzene-containing polymer series was characterized with the aim of identifying the best photoresponsive material to record a holographic vector vortex grating. The azopolymer having an oxygen substituent, as well as no methylene spacer between the main chain and the azobenzene mesogen, shows the larger photoresponse to polarized light. It seems that flexible spacer prevents a faster and higher saturation level in optical recording. Besides, it was found that low molecular weight favors a higher photoalignment rate.

By coating the glass substrate with the chosen azopolymer using the film casting method, the holographic recording medium was obtained. Two vector vortex beams, radial and azimuthal linearly polarized, were superimposed subtending a small angle on the prepared photoreactive film. The resulting holographic polarization diffractive element was then reconstructed.

6.2 Main Findings and Contributions to Knowledge

It was demonstrated, theoretically and experimentally, that a vector vortex grating can be obtained by polarization holography using a photoanisotropic polymer film as the recording medium. The optical device was optically characterized by different methods such as Stokes and Mueller imaging polarimetry, that were used to evaluate the diffracted vector fields and the photoinduced anisotropy in the polymer films, respectively. Through the decomposition of Mueller matrix in each pixel, a spatial mapping of the elementary optical anisotropies such as diattenuation, depolarization and birefringence was calculated. For the holographic reconstruction, Stokes polarimetry was implemented. In this regard, one of the two recording beams was obstructed,

illuminating with the other one and obtaining the reconstruction of the former that is being blocked. In this case, the complementary beam of that used to illuminate the hologram is being reconstructed; that is to say, the vector vortex grating was able to classify the type of incident vector beam. Another interesting result consists in the double-fork grating observed as a result of the holographic recording. Further research on the properties of this unique phase distribution should be done.

It was proven that synthesized side-chain azobenzene-containing polymers have the ability to record circular polarization, unlike other materials that only record linear polarization. The photoresponse efficiency depends on the spacer of each polymer and on the thickness of each film. This chemical structural features seems to affect also dissolution properties of the polymer powder. When the methylene spacer is larger, the polymer dissolves faster and when the spacer is smaller, the polymer dissolves slower. When the polymer dissolves faster, the solution is visibly more liquid than the polymer solution with a smaller or null spacer (POC6-0), this influences the moment of the deposition of the films, since with a longer spacer, the films, regardless of the deposition method, are thinner than films made with polymer with a smaller spacer. From this, it can be explained why films made with polymer with a larger spacer take longer to be recorded, and also their efficiency is much lower than films with polymer with a small or even null spacer; and in turn, if they are thicker films have a better holographic recording because of the retardance, which refers to the difference in phase delay experienced by two components of a polarized light beam traveling through a birefringent medium.

6.3 Practical Implications and Final Thoughts

One of the practical applications of this research consists in the possibility of recording by holographic multiplexing a number of cylindrical vector beams to use the resulting vector vortex grating as a sorter or analyzer of vector vortex beams. In this case, only two vector beams were recorded (radial and azimuthal linearly polarized) and subsequently reconstructed. However, as a future job, it is intended to record and reconstruct more than two vector vortex beams through the same method that was implemented, in this way, it can be classified more than two vector vortex beams in one holographic grating. Highlighting the photoanisotropic properties that these side-chain azobenzene-containing polymers have, which show a good response compared to those of other materials, when they are being recorded. This multiplexing has been done on

metasurfaces; however, they have only obtained an efficiency of 15.3% applying complex methods.

This research allows to report the anisotropic properties of the polymeric material by measuring the birefringence in each polymer film. Likewise, it has been demonstrated that this material has the ability to record circular polarization, unlike other materials that only records linear polarization, showing that these types of materials are more efficient in polarization holography.

Bibliography

[1] F. Weigert. "Uber Einen Neuen Effect der Strahling in Lichtempfindlichen Schichten". In: *Verh. Dtsch. Phys. Ges* 21 (1919), pp. 479–483.

[2] T. Kondo. "Uber den photoanisotropen Effekt (Weigerteffekt) an Farbstoffen I". In: *Z. Wiss. Photogr. Photophys. Photochem* 31 (1932), pp. 153–167.

[3] A. W. Lohmann. "Reconstruction of Vectorial Wavefronts". In: *Appl. Opt.* 4 (1965), pp. 1667–1668.

[4] Sh. D. Kakichashvlli. "On polarization recording of holograms". In: *Opt. Spektrosk.* 33 (1972), p. 324.

[5] Y. Zhai et al. "A Review of Polarization-Sensitive Materials for Polarization Holography". In: *Materials* 13 (2020), p. 5562.

[6] L. Nikolova and P. S. Ramanujam. *Polarization Holography*. 1st. UK: Cambridge University Press, 2009.

[7] X.Wang. *Azo Polymers: Synthesis, Functions and Applications*. 1st. Berlin: Springer, 2017.

[8] V. Ovdenko et al. "Effect of molecular weight of PEG polymer matrix on the diffraction efficiency of Methyl Orange holographic media". In: *Opt. Mater.* 111 (2021), p. 110549.

[9] M. Hendrikx et al. "Light-Triggered Formation of Surface Topographies in Azo Polymers". In: *Crystals* 7 (2017), p. 231.

[10] S. Sun et al. "Photoresponsive polymers with multiazobenzene groups". In: *Polym. Chem.* 10 (2019), p. 4389.

[11] G. Martinez-Ponce et al. "Investigations on photoinduced processes in a series of azobenzene-containing side-chain polymers". In: *J. Opt. A: Pure Appl. Opt.* 6 (2004), pp. 324–329.

[12] Chiara Fedele et al. "New tricks and emerging applications from contemporary azobenzene research". In: *Photochemical and Photobiological Sciences* 21 (2022), pp. 1719–1734.

[13] C. V. Castro-Pérez et al. "Liquid crystal and photo-induced properties of polymers carrying pyridylazobenzene groups and iodopentafluorobenzene rings self-assembled through halogen bond". In: *J. Fluor. Chem.* 222-223 (2019), pp. 90–99.

[14] C. de Santiago-Solís et al. “Liquid-crystalline and photo-induced properties of P4VP quaternized with bromo derivative of dialkyloxy-phenyleneazobenzene groups”. In: *J. Appl. Polym. Sci.* 134 (2017), p. 44819.

[15] T. García et al. “Liquid-crystalline polymers bearing phenylene(azobenzene) moieties substituted with an electron-donor or electron-acceptor lateral group. Synthesis, mesomorphic behavior and photo-induced isomerization”. In: *Polymer* 53 (2012), pp. 2049–2061.

[16] R. J. Rodríguez-Gonzalez et al. “Enhancement of the photoinduced birefringence and inverse relaxation of a liquid crystal azopolymer by doping with carbon nanostructures”. In: *J. Photochem. Photobiol. A* (2023), p. 114342.

[17] G. Martinez-Ponce et al. “All-optical switching using supramolecular chiral structures in azopolymers”. In: *J. Opt. A: Pure Appl. Opt.* 10 (2008), p. 115006.

[18] G. Martinez-Ponce et al. “Bifocal-polarization holographic lens”. In: *Opt. Lett.* 29 (2004), pp. 1001–1003.

[19] L. Nedelchev et al. “In-line and off-axis polarization-selective holographic lenses recorded in azopolymer thin films via polarization holography and polarization multiplexing”. In: *Appl. Opt.* 62 (2023), pp. D1–D7.

[20] G. Sudesh Kumar and D.C. Neckers. “Photochemistry of azobenzene-containing polymers”. In: *Chem. Rev.* 8.89 (1989), pp. 1915–1925.

[21] C. Cojocariu and P. Rochon. “Photochemistry of azobenzene-containing polymers”. In: *Pure Appl. Chem.* 76 (2004), pp. 1479–1497.

[22] K. Ichimura. *Photochromic and Thermochromic Compounds*. 1st. New York: Kluwer Academic/Plenum, 1999.

[23] K. Ichimura. *Photochromism: Molecules and Systems*. 1st. Amsterdam: Bouas-Laurent, H. Ed., 1990.

[24] J. del Barrio and C. Sánchez-Somolinos. “Light to Shape the Future: From Photolithography to 4D Printing”. In: *Adv. Optical Mater* 7 (2019), p. 1900598.

[25] Firebird Optics. *An introduction to Diffracting Gratings*. 2023. URL: https://www.firebirdoptics.com/blog/an-introduction-to-diffraction-gratings.

[26] H. M. D. Bandara and S. C. Burdette. “Photoisomerization in different classes of azobenzene”. In: *Chem. Soc. Rev.* 41 (2012), pp. 1809–1825.

[27] H. Rau. *Photochemistry and Photophysics*. 1st. CRC Press, 1990.

[28] M. Ribagorda and E. Merino. “Fotoisomerización de azobencenos: movimientos moleculares a la carta”. In: *An. Quím.* 4.105 (2009), pp. 290–299.

[29] B. Blagoeva et al. “Reversible supramolecular chiral structures induced in azopolymers by elliptically polarized light: influence of the irradiation wavelength and intensity”. In: *Appl. Opt.* 61 (2022), B147–B155.

[30] G. Martinez-Ponce. "Mueller imaging polarimetry of holographic polarization gratings inscribed in azopolymer films". In: *Opt. Express* 24 (2016), pp. 21364–21377.

[31] K. Ichimura. "Photoalignment of Liquid-Crystal Systems". In: *Chem. Rev.* 100 (2000), pp. 1847–1873.

[32] C. Cojocariu and P. Rochon. "Light-induced motions in azobenzene- containing polymers". In: *Pure Appl. Chem.* 76.7-8 (2004), pp. 1479–1497.

[33] E. Bagherzadeh-Khajeh Marjan et al. "Cyano azobenzene polymer films: Photo-induced reorientation and birefringence behaviors with linear and circular polarized light". In: *Optical Materials* 38 (2004), pp. 228–232.

[34] A. Kozanecka-Szmigiel et al. "Photoinduced birefringence of azobenzene polymer at blue excitation wavelengths". In: *Appl. Phys. B* 119 (2015), pp. 227–231.

[35] N Hosono et al. "Large-area three-dimensional molecular ordering of a polymer brush by one-step processing". In: *Science* 330 (2010), pp. 808–811. DOI: 10.1126/science.1195302.

[36] Boaz Jessie Jackin et al. "Compact and Scalable Large Vortex Array Generation Using Azocarbazole Polymer and Digital Hologram Printing Technique". In: *Nanoscale Research Letters* 17 (2022), p. 44. DOI: 10.1186/s11671-022-03675-7.

[37] William A. Shurcliff and Stanley S. Ballard. *Polarized Light*. Commission on College Physics, 1964.

[38] Dennis H. Goldstein. *Polarized Light*. CRC Press, 2011. DOI: 10.1201/b10436.

[39] Arun Kumar and Ajoy Ghatak. *Jones Vector Representation of Polarized Light*. SPIE Press, 2011. DOI: 10.1117/3.861761.ch5.

[40] Xizheng Ke. *Generation, Transmission, Detection, and Application of Vortex Beams*. Springer, 2023.

[41] Qiwen Zhan. "Cylindrical vector beams: from mathematical concepts to applications". In: *Advances in Optics and Photonics* 1 (2009), pp. 1–57.

[42] Praveen Kumar et al. "Self-referenced interferometry for single-shot detection of vector-vortex beams". In: *Scientifc Reports* 12 (2022), p. 17253.

[43] J. Qi et al. "Practical generation of arbitrary high-order cylindrical vector beams by cascading vortex half-wave plates". In: *Optics Express* 29 (2021), pp. 25365–25376.

[44] Masaaki Sakakura et al. "Ultralow-loss geometric phase and polarization shaping by ultrafast laser writing in silica glass". In: *Light: Science and Applications* 9 (2020), p. 15.

[45] Martynas Beresna, Mindaugas Gecevicius, and Peter G. Kazansky. "Polarization sensitive elements fabricated by femtosecond laser nanostructuring of glass". In: *Optical Materials Express* 1 (2011), pp. 783–795.

[46] L. Nikolova et al. "Self-induced light polarization rotation in azobenzene-containing polymers". In: *Appl. Phys. Lett.* 77 (2000), pp. 657–659. DOI: 10.1063/1.127076.

[47] S. Pages et al. "Photoinduced linear and/or circular birefringences from light propagation through amorphous or smectic azopolymer films". In: *Appl. Phys. B* 75 (2002), pp. 541–548. DOI: 10.1007/s00340-002-0976-7.

[48] Richard Barakat. "Exponential versions of the Jones and Mueller-Jones polarization matrices". In: *J. Opt. Soc. Am. A* 13 (1996), pp. 158–163. DOI: 10.1364/JOSAA.13.000158.

[49] R. Clark Jones. "A New Calculus for the Treatment of Optical Systems. VII. Properties of the N-Matrices". In: *J. Opt. Soc. Am.* 38 (1948), pp. 671–685. DOI: 10.1364/JOSA.38.000671.

[50] L. Nikolova et al. "Polarization holographic gratings in side-chain azobenzene polyesters with linear and circular photoanisotropy". In: *Appl. Opt.* 35 (1996), pp. 3835–3840. DOI: 10.1364/AO.35.003835.

[51] I. Naydenova et al. "Polarimetric investigation of materials with both linear and circular anisotropy". In: *J. Mod. Opt.* 44 (1997), pp. 1643–1650. DOI: 10.1080/09500349708230764.

[52] Moritsugu Sakamoto et al. "Polarization grating fabricated by recording a vector hologram between two orthogonally polarized vector vortex beams". In: *J. Opt. Soc. Am. B* 34 (2017), pp. 263–269. DOI: 10.1364/JOSAB.34.000263.

[53] R. J. Rodriguez-Gonzalez et al. "Optical and Liquid Crystalline Properties of New Alkyl-Substituted Azopolymers". In: *Mol. Cryst. Liq. Cryst* 511 (2009), 283/[1753]–291/[1761].

[54] Z. Sekkat and W Knoll. "Photoreactive Organic Thin Films". In: *Academia Press* (2002).

[55] R. J. Sension et al. "Femtosecond laser studies of the cis-stilbene photoisomerization reactions". In: *J. Chem. Phys.* 98 (1993), pp. 6291–6315.

[56] T. Nägele et al. "Photoisomerization in Different Classes of Azobenzene". In: *Chem. Phys. Lett.* 272 (1997), pp. 489–495.

[57] N. Holme, P. Ramanujam, and S. Hvilsted. "10,000 optical write, read, and erase cycles in an azobenzene sidechain liquid-crystalline polyester". In: *Optics Letters* 21 (1996), pp. 902–904. DOI: 10.1364/ol.21.000902.

[58] Denis Constales, Gregory S. Yablonsky, and Guy B. Marin. *Advanced Data Analysis and Modelling in Chemical Engineering*. Elsevier, 2017.

[59] Nobuhiro Kawatsuki et al. "Reversion of Alignment Direction in the Thermally Enhanced Photoorientation of Photo-Cross-Linkable Polymer Liquid Crystal Films". In: *Macromolecules* 35 (2001), pp. 706–713. DOI: 10.1021/ma011439u.

[60] Ljiljana Janicijevic and Suzana Topuzoski. "Fresnel and Fraunhofer diffraction of a Gaussian laser beam by fork-shaped gratings". In: *Journal of the Optical Society of America A* 25 (2008), pp. 2659–2669. DOI: 10.1364/JOSAA.25.002659.

[61] Mohammad Reza Rashidian Vaziri et al. “A simple method to prepare and characterize optical fork-shaped diffraction gratings for generation of orbital angular momentum beams”. In: *Journal of Optics* To be assigned (2024). DOI: 10.1007/s12596-024-02154-9.

[62] Shih Yau Lu and Russell A. Chipman. “Interpretation of Mueller matrices based on polar decomposition”. In: *Journal of the Optical Society of America A* 13 (1996), pp. 1106–1113. DOI: 10.1364/JOSAA.13.001106.